Functional analysis of cold shock proteins from an extreme thermophile, *Thermus thermophilus* HB8

Doctoral Thesis

2010. 3

Ryosuke Mega

Graduate School of Frontier Biosciences, Osaka University

CONTENTS

Abbreviations

CIP	cold-induced protein
CSP	cold shock protein
CSD	cold shock domain
ssDNA	single-stranded DNA
ssRNA	single-stranded RNA
dsDNA	double-stranded DNA
ttCSP1	a cold shock protein (TTHA0175) of *T. thermophilus* HB8
ttCSP2	a cold shock protein (TTHA0359) of *T. thermophilus* HB8
E. coli Csp	ecCsp
B. caldolyticus Csp	bcCsp
EMSA	electrophoretic mobility shift assay
PMSF	phenylmethanesulfonyl fluoride
MALDI-TOF	matrix-assisted laser desorption-ionization time-of-flight
MS	mass spectrometry
IPTG	isopropyl β-D-thiogalactoside
Δ*ttha0252*	*ttha0252* deletion strain
Δ*ttcsp1*	*ttcsp1* deletion strain
Δ*ttcsp2*	*ttcsp2* deletion strain
Δ*ttcsp1/2*	*ttcsp1 ttcsp2* double deletion strain
K_d	the dissociation constant
5'-UTR	5'-untranslated region
SD	Shine-Dalgarno

Summary

A rapid downshift in temperature induces the expression of a specific set of proteins. Cold-shock induction is known to be regulated at the transcriptional, post-transcriptional and translational levels. I focused on cold-induction of two cold shock proteins, termed as ttCSP1 and ttCSP2 in *Thermus thermophilus* HB8. DNA microarray analysis indicated that the mRNA expression level of *ttcsp2* was dramatically increased compared with that of *ttcsp1* which was constitutively expressed in *Thermus thermophilus* HB8. Surprisingly, *ttcsp2* induction occurred immediately (30 s) after temperature downshift. However, ttCSP2 protein expression was observed at 30 min after temperature downshift. Such a time lag between the mRNA and protein expression suggested that expression of ttCSP2 was controlled at the translational level. The *ttcsp2* mRNA 5'-untranslated region was predicted to form the stable secondary structure at lower temperature. This suggested that the stability of *ttcsp2* mRNA was involved in the temperature-dependent expression in the cell. Gene disruption experiments showed that at least one CSP was necessary for normal growth under cold conditions, suggesting that ttCSP1 could compensate for the lack of ttCSP2 and *vice versa*. DNA microarray analysis of the *ttcsp2* disruptant showed up- and down-regulation of many genes, which were different from that of the *ttcsp1* disruptant. Nucleotide binding assay indicated that ttCSP1 bound to single-stranded DNA forming secondary structure more strongly than ttCSP2 did. DNA-melting activity was observed only in ttCSP1. ttCSP1 and ttCSP2 structures indicated ttCSP1 had the positively charged region near the putative oligonucleotide-binding site, whereas ttCSP2 did not. These results suggested that both ttCSP1 and ttCSP2 act as transcriptional regulators for different genes in a distinct manner under different growth conditions.

Introduction

All organisms have multiple systems to adapt to various environmental changes. An abrupt downshift in growth temperature, termed as cold shock, is one of environmental stresses. Temperature downshift affects cells as follows: (i) decrease in membrane fluidity to affect the membrane-associated functions such as active transport and secretion; (ii) stabilization of secondary structure of nucleic acids leading to reduced efficiency of mRNA transcription and translation; (iii) slow or inefficient folding of some proteins; and (iv) inhibition of ribosome function (Graumann and Marahiel, 1996; Phadtare, 2004). A cold adaptation system exists to overcome these negative influences of exposure to cold stress in all organisms.

The studies involved in cold shock response have been performed in various industries such as food, agriculture and research as shown in Table 1. For example, understanding cold shock response of food-borne pathogens such as *Listeria* and *Salmonella* is useful for food storage because a commonly used method is refrigeration. Development of agricultural biotechnologies such as breeding cold-tolerant crop is required for stable supply of

Table 1. Commercial significance of study of cold-shock response.

Industry	Concern	Solution
Food	Spoilage of refrigerated food and infections due to food-borne pathogens	Reduce efficiency of cold- shock response of food- borne pathogens
	Instability of lactic acid bacteria starter cultures due to temperature changes during fermentations in dairy industry	Modify starter cultures to improve cold adaptation and cryotolerance
Agriculture	Reduced efficiency of 'biofertilizers' due to low temperatures	Use of cold-adapted Rhizobial cultures
	Great economic losses due to low tolerance of plants to low temperatures	Enhance chilling resistance of plants using gene transfer from bacteria to plants
Research	Inefficient expression of proteins due to temperature sensitivity or proteolysis	Cold-inducible expression systems for production of these proteins
	Reduced efficiency of certain processes using biocatalysts at low temperatures	Use of cold-adapted enzymes

This table is from Phadtare (2004).

agricultural products in the environment exposed to cold weather. These technologies can lead to improve the agricultural production in the cold region. However, though several factors involved in cold shock response have been reported, detailed molecular mechanism about cold response of living organism remains to be mysterious. Thus, revealing the cold response mechanism of living organism contributes to resolve issues described above.

The cold response has been studied extensively in *Escherichia coli* and *Bacillus subtilis*. Control of the cold response occurs at the transcriptional, post-transcriptional and translational levels. In these mesophiles, cold response in terms of mRNA expression have been examined over a time range of 10 min to several hours (Gualerzi et al., 2003). To reveal how bacteria sense the change in temperature, initial stage of cold shock response must be investigated in more detail. Moreover, very little is known concerning the regulation of the cold shock response in other bacterial species. I reasoned that studying the cold shock response of a thermophilic bacterium might be useful in gaining a greater understanding of this phenomenon. Here, I focused on bacterial cold response at earlier stage and performed DNA microarray analysis at 0.5 and 10 min after cold shock.

Upon a downshift in temperature, many proteins, termed as cold-induced proteins (CIPs), are induced, whereas many proteins that are synthesized under normal growth conditions are repressed (Fig. 1) (Phadtare, 2004). Some of CIPs are required for various cellular activities including metabolism, transcription, translation and protein folding under cold condition (Graumann and Marahiel, 1996; Gualerzi et al., 2003). A cold shock protein (CSP) was identified as one of CIPs, and its homologues possess a cold shock domain (CSD) including RNP1 and RNP2 motifs (Fig. 2). These motifs are highly conserved in single-stranded DNA (ssDNA) and single-stranded RNA (ssRNA)-binding proteins (Horn et al., 2007). It is hitherto reported that CSPs function as RNA chaperone to inhibit mRNA secondary structure

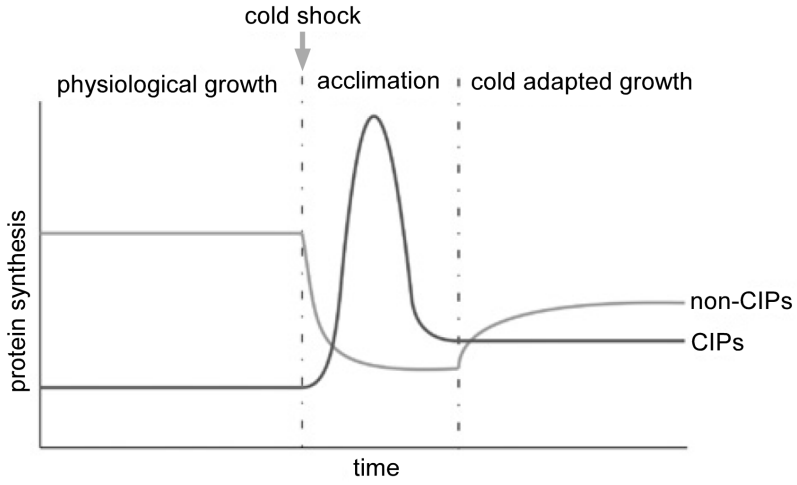

Fig. 1. Expression pattern of cold-induced proteins (CIPs) and non-CIPs. This figure is cited from Horn *et al.* (2007).

```
                                RNP1          RNP2
ttCSP1     1 MQ---KGRVKWFNAEKGYGFIERE-GDTDVFVHYTAINAKG----FRTLNEGDIVTFDVEPGRNGKGPQAVNVTVVEPARR-- 73
ttCSP2     1 MN---KGIVKWFNAEKGYGFIQQE-EGPDVFVHFSAIEADG----FRTLSEGERVEFEVEPGRNGKGPQARRVRRL------ 68
ecCspA     1 MSGKMTGIVKWFNADKGFGFITPDDGSKDVFVHFSAIQNDG----YKSLDEGQKVSFTIESGA--KGPAAGNVTSL------- 70
ecCspB     1 MSNKMTGLVKWFNADKGFGFISPVDGSKDVFVHFSAIQNDN----YRTLFEGQKVTFSIESGA--KGPAAANVIITD------ 71
ecCspC     1 MA-KIKGQVKWFNESKGFGFITPADGSKDVFVHFSAIQGNG----FKTLAEGQNVEFEIQDGQ--KGPAAVNVTAI------- 69
ecCspD     1 ME---KGTVKWFNNAKGFGFICPEGGGEDIFAHYSTIQMDG----YRTLKAGQSVQFDVHQGP--KGNHASVIVPVEVEAAVA 74
ecCspE     1 MS-KIKGNVKWFNESKGFGFITPEDGSKDVFVHFSAIQTNG----FKTLAEGQRVEFEITNGA--KGPSAANVIAL------- 69
ecCspF     1 MSRKMTGIVKTFDGKSGKGLITPSDGRIDVQLHVSALNLRD----AEEITTGLRVEFCRINGL--RGPSAANVYLS------- 70
ecCspG     1 MSNKMTGLVKWFNADKGFGFITPDDGSKDVFVHFTAIQSNE----FRTLNENQKVEFSIEQGQ--RGPAAANVVTL------- 70
ecCspH     1 MSRKMTGIVKTFDRKSGKGFIIPSDGRKEVQVHISAFTPRD----AEVLIPGLRVEFCRVNGL--RGPTAANVYLS------- 70
ecCspI     1 MSNKMTGLVKWFNPEKGFGFITPKDGSKDVFVHFSAIQSND----FKTLTENQEVEFGIENGP--KGPAAVHVVAL------- 70
bsCspB     1 ML---EGKVKWFNSEKGFGFIEVEGQD-DVFVHFSAIQGEG----FKTLEEGQAVSFEIVEGN--RGPQAANVTKEA------ 67
bsCspC     1 ME---QGTVKWFNAEKGFGFIERENGD-DVFVHFSAIQSDG----FKSLDEGQKVSFDVEQGA--RGAQAANVQKA------- 66
bsCspD     1 MQ---NGKVKWFNNEKGFGFIEVEGGD-DVFVHFTAIEGDG----YKSLEEGQEVSFEIVEGN--RGPQASNVVKL------- 66
stCSPA     1 MSGKMTGIVKWFNADKGFGFITPDDGSKDVFVHFSAIQNDG----YKSLDEGQKVSFTIESGA--KGPAAGNVTSL------- 70
mtCSPA     1 MP---QGTVKWFNAEKGFGFIAPEDGSADVFVHYTEIQGTG----FRTLEENQKVEFEIGHSP--KGPQATGVRSL------- 67
mlCSPA     1 MA---VGTVKWFNAEKGYGFIAPEDNSADVFVHFSAIQGNG----FKELQENDRVEFETQDGP--KGLQAANVTKL------- 67
lmCSPA     1 ME---QGTVKWFNAEKGFGFIERENGD-DVFVHFSAIQGDG----FKSLDEGQAVTFDVEEGQ--RGPQAANVQKA------- 66
spCSPA     1 MA---QGTVKWFNAEKGFGFISTENGQ-DVFAHFSAIQTNG----FKTLEEGQKVAFDVEEGQ--RGPQAVNITKLA------ 67
paCSPA     1 MSNRQNGTVKWFNDAKGFGFITPESGN-DLFVHFRSIQGTG----FKSLQEGQKVSFVVVNGQ--KGLQADEVQVV------- 69
ypCSPB     1 MSNKMTGLVKWFDAGKGFGFISPADGSKDVFVHFSAIQGND----YKTLDEGQNVEFSIEQGQ--KGPSAVNVVAL------- 70
hiCSPD     1 ME---IGIVKWFNNAKGFGFISAEGVDADIFAHYSVIEMDG----YRSLKAGQKVQFEVLHSD--KGSHATKIIPIADTQE-- 72
YB-1      58 ---KVLGTVKWFNVRNGYGFINRNDTKEDVFVHQTAIKKNNPRKYLRSVGDGETVEFDVVEGE--KGAEAANVTGP------ 128
DBPA      90 ----VLGTVKWFNVRNGYGFINRNDTKEDVFVHQTAIKKNNPRKYLRSVGDGETVEFDVVEGE--KGAEAANVTGP------- 160
UNR      185 ---RCQGVVCAMK--EAFGFIERGDVVKEIFFHYSEFKGDL-----ETLQPGDDVEFTIKDRN--GKEVATDVRLL------- 248
CRHSP     62 VY---KGVCKCFCRSKGHGFITPADGGPDIFLHISDVEGEY------VPVEGDEVTYKMCSIPP-KNEKLQAVEVVIT----- 129
LIN-28    52 RY---FGSCKWFNVSKGYGFVIDDITGEDLFVHQSNLNMQG----FRSLDEGERVSYYIQERSNGKGREAYAVSGE------- 120
                 *    :   .. *::       ::  *   .             .  * :             :
```

Fig. 2. Amino acid sequence alignment of CSP homologues and cold shock domains from different proteins. Amino acid sequences are from *T. thermophilus* HB8 (tt), *Escherichia coli* (ec), *Bacillus subtilis* (bs), *Salmonella typhimurium* (st), *Mycobacterium tuberculosis* (mt), *Micrococcus luteus* (ml), *Listeria monocytogenes* (lm), *Streptococcus pyogenes* (sp), *Pseudomonas aeruginosa* (pa), *Yersinia pestis* (yp), *Haemophilus influenzae* (hi). YB-1, DBPA, UNR and CRHSP are derived from human. LIN-28 is from *Caenorhabditis elegans*. Sequences were aligned using the program ClustalW (Thompson et al., 1994). Identical, highly conserved and weakly conserved residues are indicated by asterisks, colons and periods, respectively.

formation (Fig. 3) (Jiang et al., 1997; Max et al., 2006). Also, CSPs are thought to enhance mRNA degradation and translation efficiency (Graumann and Marahiel, 1996). Some CSPs are known to unwind the RNA secondary structures and act as a transcriptional antiterminator (Bae et al., 2000; Phadtare et al., 2002a). RNA degradation mediated by exoribonuclease and endoribonuclease are also activated by CSPs (Awano et al., 2008). These studies suggest that CSPs are likely to inhibit the formation of mRNA secondary structures which act as a terminator as well as being involved in mRNA regulation by ribonucleases.

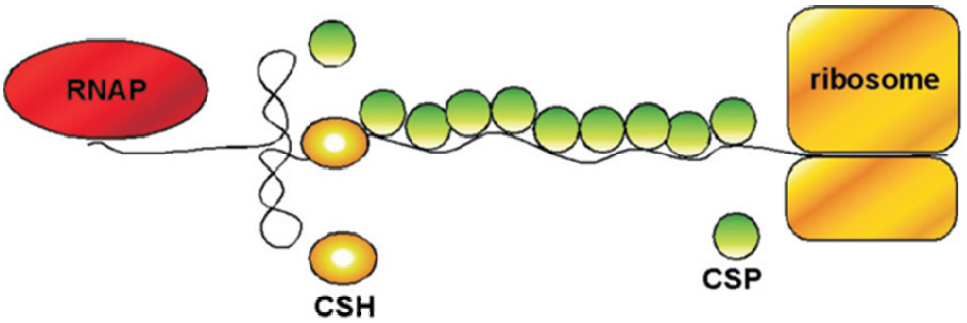

Fig. 3. RNA chaperone activity of CSP. RNAP and CSH represent RNA polymerase and cold-inducible RNA helicase, respectively. This figure is cited from El-Sharoud and Graumann (2007).

Most organisms possess multiple kinds of CSPs (Table 2). Particularly, *E. coli* has nine CSP homologues which are named in alphabetical order from CspA to CspI (Yamanaka et al., 1998). CspA, CspB, CspG and CspI were found to be cold-inducible (Lee et al., 1994; Nakaminami et al., 2006; Wang et al., 1999). CspC and CspE underwent constitutive expression pattern at both high and low temperature (Yamanaka et al., 1994). CspD expressed during stationary phase and upon nutrient starvation (Yamanaka and Inouye, 1997). These observations suggest that CSP homologues function under normal growth and stress as well as cold condition. It is interesting that the functional condition is different despite

Table 2. Distribution of *E. coli* CspA (ecCspA) homologues. Homologues of ecCspA were searched by using NCBI BLAST. The homologues with E-value < 0.1 are listed. In eukaryota, the proteins with CSD were regarded as these homologues. *T. thermophilus* was marked with asterisk.

Bacteria	Species	CspA homologues
Aquificae	*Aquifex aeolicus*	1
	Hydrogenivirga	2
Actinobacteria	*Arthrobacter aurescens*	4
	Mycobacterium tuberculosis	2
Chlamydiae	*Chlamydia trachomatis*	0
Chlorobi	*Chlorobium phaeobacteroides*	3
	Pelodictyon luteorum	2
Cyanobacteria	*Nodularia spumigena*	1
	Synechocystis sp. PCC6803	0
Deinococcus	*Deinococcus radiodurans*	1
-Thermus	*Thermus thermophilus*	2*
Firmicutes	*Bacillus subtilis*	3
	Lactobacillus casei	4
Mollicutes	*Acholeplasma laidlawii*	1
	Mycoplasma pneumoniae	0
Proteobacteria		
alpha	*Methylobacterium radiotolerans*	6
	Rhodobacter sphaeroides	7
beta	*Bordetella avium*	5
	Nitrosomonas europaea	4
gamma	*Escherichia coli*	9
	Pseudomonas aeruginosa	7
delta	*Geobacter sulfurrenducens*	4
	Pelobacter carbinolicus	5
epsilon	*Acrobacter butzleri*	1
	Helicobacter pylori	0
Spirochaetes	*Treponema pallidum*	0
Thermotogae	*Thermotoga maritima*	3

Archaea	Species	CspA homologues
Crenarchaeota	*Cenarchaeum symbiosum*	1
	Sulfolobus solfataricus	0
Euryarchaeota	*Halobacterium sarinarum*	2
	Methanocaldococcus jannaschii	0

Eukaryota	Species	CspA homologues
Alveolata	*Cryptosporidium parum*	1
	Plasmodium berghei	1
Euglenozoa	*Leishmania braziliensis*	1
	Trypanosoma brucei	1
Fungi	*Aspergillus clavatus*	1
	Saccharomyces cerevisiae	0
Metazoa	*Caenorhabditis elegans*	8
	Homo sapiens	28
	Mus musculus	43
Viridiplantae	*Arabidopsis thaliana*	5
	Oryza sativa	6

amino acid sequence of CSPs is very similar among the homologues. Also, *E. coli* CspE (ecCspE) compensated for triple-deletion of CspA, CspB and CspG and ecCspE expression level increased at low temperature (Xia et al., 2001). This observation suggests that the function of these homologues may overlap and they are able to substitute mutual function under cold condition. However, many CSP homologues in one species can be a barrier for the cellular functional analysis because of their mutual compensation. Thus, *Thermus thermophilus* HB8 which has two CSP homologues, termed as ttCSP1 (TTHA0175) and ttCSP2 (TTHA0359) is a useful model organism for studying the functional differentiation of CSPs.

In this research, I studied on the biochemical and molecular biological analyses of cold shock proteins from *T. thermophilus* HB8. DNA microarray analysis revealed that the mRNA expression level of ttCSP2 was dramatically increased compared with that of ttCSP1 which was constitutively expressed. Surprisingly, this induction occurred immediately (30 s) after temperature downshift. However, expression of ttCSP2 protein was observed at 30 min. This time lag between mRNA and protein expression suggests that expression of ttCSP2 is controlled at the translational level. Nevertheless, I concluded that ttCSP2 was a cold-inducible CSP of *T. thermophilus* HB8.

Then, to investigate how *ttcsp2* mRNA expression increased dramatically, transcription start site of *ttcsp2* mRNA was determined and the secondary structure in 5'-untranslated region (5'-UTR) was predicted at 70˚C and 45˚C. Interestingly, the secondary structure forming in 5'-UTR was likely to be very different between before and after cold shock. This temperature-dependent secondary structure could affect the stability of *ttcsp2* mRNA in the cell. Also, this structure sequestered Shine-Dalgarno (SD) like sequence. This was suggested to be a reason causing the time lag between mRNA and protein expression of *ttcsp2*.

In addition, abundance of *ttcsp2* mRNA increased in deletion mutant strain of TTHA0252, which has 5'-3' exoribonuclease and endoribonuclease activity at 70˚C. This suggested that *ttcsp2* mRNA was regulated by TTHA0252. Thus, it is possible that the temperature-dependent secondary structure in 5'-UTR control translation as well as transcripts of *ttcsp2*.

I constructed each single gene disruptant (Δ*ttcsp1* and Δ*ttcsp2*) and a double disruptant (Δ*ttcsp1/2*) of *T. thermophilus* HB8. Consequently, growth of Δ*ttcsp1/2* was significantly delayed compared with the other strains (wild-type, Δ*ttcsp1* and Δ*ttcsp2*). These results suggested that ttCSP1 could compensate for the lack of ttCSP2 and *vice versa* under cold condition. Thus, either *ttcsp1* or *ttcsp2* are necessary for normal growth at low temperature. In addition, I performed DNA microarray by using Δ*ttcsp2* and found the candidates of target genes regulated by ttCSP2 such as cell wall / membrane biogenesis (M, *ttha0641-0648*), survival proteins (*ttha0360-0363*) and amino acid transporter (*ttha0447-0452*).

By *in vitro* assay, ttCSP1 and ttCSP2 displayed a higher affinity for ssDNA with thymine than any other base and showed tighter binding as the length of the DNA molecule increased. In particular, ttCSP1 bound to ssDNA containing secondary structure more strongly than ttCSP2 did. The crystal structure of ttCSP1 and a model structure of ttCSP2 suggested the difference in the ability of these proteins to recognize stem-loop structure. Our results suggest that both ttCSP1 and ttCSP2 act as an RNA chaperone, but ttCSP1 functions as a transcription antiterminator.

In conclusion, this study provides some clues to a molecular mechanism of cold adaptation through a functional differentiation between these two cold shock proteins.

Materials and Methods

1. Materials

DNA microarray data of Δ*ttha0252* was provided from Harima RIKEN. All strains were derivatives of *T. thermophilus* HB8 (ATCC27634). The oligonucleotides were synthesized by BEX Co (Tokyo, Japan). All other reagents used were of the highest commercially available grade.

2. DNA microarray analysis.

The *T. thermophilus* HB8 wild-type strain was cultured at 70°C until OD_{600} in TT medium reached 0.8 (Hashimoto et al., 2001). The culture was then divided into two flasks and an equal volume of hot or cold medium added. Each diluted culture was collected into equal volume of 100% ethanol at 0 and 10 min after cultivating at 70°C or 45°C and stored at -80°C. Total RNA was extracted from these frozen cells by following basically the same procedure as that described previously with the exception that the RNA was re-suspended in 20 μl of water after ethanol precipitation (Shinkai et al., 2007).

cDNA was synthesized with SuperScript II (Invitrogen, Carlsbad, CA, USA) reverse transcriptase in the presence of the RNase inhibitor SUPERase (Ambion, Austin, TX, USA) and 6-base random primers (Invitrogen). The cDNA was fragmented with 35 units DNase I (GE Healthcare UK) at 37°C for 10 min; after inactivation at 98°C for 10 min, the cDNA fragments were labeled with the GeneChip DNA labeling reagent (Affymetrix, Santa Clara, CA, USA), using terminal transferase, according to the manufacturer's instructions (Affymetrix).

The 3'-terminally labeled cDNA (2 μg) was hybridized to a TTHB8401a520105F

GeneChip (Affymetrix), which contained probe sets of 25-mer oligonucleotides representing 2238 ORFs and 1096 intergenic regions. The procedure used was basically the same as that described previously with the exception that 20 μg of herring sperm DNA (Promega) was added (Shinkai et al., 2007). The array was automatically washed and stained with streptavidin-phycoerythrin (Invitrogen) using a GeneChip Fluidics Station 450XP (Affymetrix). The probe array was scanned with a GeneChip Scanner 3000 (Affymetrix). To determine the mRNA expression level at 45°C after cold shock relative to that at 70°C, the image data for the three samples at each temperature and time point were processed.

The expression intensity of each of the 2238 ORFs for the three wild-type strains was evaluated using image data and scaled by means of the one-step Tukey's biweight algorithm using GeneChip Operating Software version 1.0 (Affymetrix). Scaled probe value (scaled intensity in Fig. 6 and 10) was calculated as $Sc = 500$ according to Statistical Algorithms Description Document (Affymetrics). The intensity data sets for each time point were normalized by the following three steps using the GeneSpring GX 7.3.1 program: data transformation (set measurements of less than 0.01 to 0.01), per chip normalization (normalize to 50th percentile), and per gene normalization (with the wild-type data at 70°C at 0 min (Agari et al., 2008). The false discovery rate (q value) (Storey and Tibshirani, 2003) of the observed differences in the normalized intensities between 70°C and 45°C was calculated using the R program (http://cran.us.r-project.org/).

3. Protein expression analysis.

The *T. thermophilus* HB8 wild-type strain for this experiment was harvested with the same method as DNA microarray analysis. The frozen cells were suspended in 1 × PBS buffer containing 1 mM phenylmethanesulfonyl fluoride (PMSF) and 5 mM EDTA. The

cells were broken by ultrasonication and centrifuged at 20,000 *g* for 20 min at 4°C. The supernatants were collected and contained amount of proteins was determined by the Bradford method. Contaminated DNA and RNA were removed from the quantified samples by using 10 U of DNase I and 5 μg of RNase A. Ice-cold acetone was added to the mixtures and incubated at -20°C over night. Then, these mixtures were centrifuged at 7,000 *g* for 10 min and the supernatants were removed. This wash procedure was repeated three times with centrifugation at 10,000 and 16,000 *g*. The pellets were then dried at room temperature and resuspended with Tris-Tricine SDS-PAGE dye. A 200 μg aliquot of each sample was subjected to Tris-Tricine SDS-PAGE (Schagger and von Jagow, 1987). Protein bands identified by peptide mass fingerprinting using MALDI-TOF MS (Bruker Daltonics, Billerica, MA, USA) are highlighted (Fig. 7B and C).

4. Primer extension assay

Primer extension assay was carried out with ttha0359_rv primer (Table 3), which is complementary to the *ttcsp2* mRNA in total RNA at 45°C at 10 min after cold shock. The primer extension product was synthesized with 500 μM dNTP mixture containing 2.5 μM [α-^{32}P]dCTP (10 μCi) by using 300 units SuperScript II reverse transcriptase (Invitrogen, Carlsbad, CA, USA) in the presence of the RNase inhibitor SUPERase (Ambion, Austin, TX, USA). This total RNA (2 μg) was used as template in this reaction. The pT7Blue vector (Novagen, Darmstadt, Germany), into which was introduced the PCR product amplified with ttha0359_rv and 0359_fw primer (Table 3), was used as the sequencing template. The sequencing product was obtained by dideoxy sequencing reaction with the sequencing template and T7 sequencing kit (usb, Cleveland, Ohio, USA) according to manufacturer's protocol. These products were analyzed on a 6% polyacrylamide-8M urea electrophoresis

denaturing gel. The gels were placed in contact with an imaging plate to visualize the bands by using BAS2500 imaging analyzer (FUJIFILM, Tokyo, Japan).

5. Prediction of mRNA secondary structure

Secondary structure in 5'-UTR of *ttcsp2* mRNA was predicted by using vsfold5 (RNA pseudonot prediction server, http://www.rna.it-chiba.ac.jp/~vsfold/vsfold5/) at 70˚C and 45˚C based on the transcription start site of *ttcsp2* mRNA determined by primer extension assay.

6. Disruption of *ttcsp1* and *ttcsp2* genes

The gene null mutants of *T. thermophilus* HB8 were constructed by using a homologous recombination method (Hashimoto et al., 2001). The plasmids for gene disruption were derivatives of pGEM-T (Promega, Tokyo, Japan) constructed by introducing a thermostable kanamycin nucleotidyltransferase gene (*htk*) (Hoseki et al., 1999) flanked by approximately 500 base pairs of DNA upstream and downstream of the *ttcsp1* and *ttcsp2* genes. For the double gene knockout, a thermostable hygromycin-B kinase gene (*hyg*) was used for the disruption of the *ttcsp2* gene (Ooga et al., 2009). The wild-type strain of *T. thermophilus* HB8 was cultured in TT medium containing 0.4 mM $MgCl_2$ and 0.4 mM $CaCl_2$. When the OD_{600} value of the culture reached 0.5, 0.4 ml of the culture was incubated with 1 μg of the deletion constructs for 4 h, and transformants were isolated by positive selection on TT plates (TT medium containing 1.5 % Phytagel (Sigma-Aldrich Co.), 1.5 mM $MgCl_2$, and 1.5 mM $CaCl_2$) containing 50 μg/ml kanamycin or 20 μg/ml hygromycin-B. To verify deletion of the target gene in the chromosomal DNA, genomic PCR and Southern blotting was performed. Primers in genomic PCR were shown in Table 3.

Table 3. Primer list for primer extension assay and genomic PCR

Name	Sequence	Length
ttha0359_rv	CTGGATGAAACCGTAGCCTTTTT	23
0175_fw	GGACCTCTTTGACCTCTTCTTCCA	24
htk_rv_2	TGAACCCCATTCCAGAAATTCTCTA	25
0359_fw	ACCTCATGGACACCACGGGGCTGGC	25
hyg_rv_2	CCGTTCACCAAGCTCTGATAGAGTT	25

7. Growth analysis

Four kinds of *T. thermophilus* HB8 strains were cultured in TT medium at 70°C until OD_{600} = 0.8 and an equal volume of cold media were added. Then, these cold-shocked cultures were cultivated at 45°C. The OD_{600} of the culture was measured.

8. Overexpression and purification of ttCSP1 and ttCSP2

The pET-11a/*ttcsp2* expression vector was used to transform *E. coli* BL21(DE3) cells (Novagen). The transformed cells were cultured at 37°C until achieving 1.0×10^8 cells in 1.5 l of LB medium containing 50 μg/ml ampicillin. Then, 1 mM isopropyl β-D-thiogalactoside (IPTG) was added and the culture was further incubated for 6 h. The cells were harvested by centrifugation at 13,000 *g* and stored at -20°C.

The frozen cells overexpressing ttCSP2 were thawed, resuspended in buffer A (50 mM Tris-HCl, 50 mM KCl, 1 mM EDTA and 5 mM 2-mercaptoethanol, pH 8.0), and then disrupted by ultrasonication for 5 min on ice. The cell lysate was centrifuged at 38,000 *g* for 60 min at 4°C. All of the following procedures were performed at 4°C. The resultant supernatant was loaded onto a Toyopearl SuperQ-650M (Tosoh, Tokyo, Japan) column equilibrated with buffer A. The column was then washed with buffer A and the unbound fraction was collected. These fractions were loaded onto a hydroxyapatite (Nacalai tesque,

Kyoto, Japan) column equilibrated with buffer B (50 mM potassium phosphate, 100 mM KCl, 1 mM 2-mercaptoethanol and 1 mM EDTA, pH 7.1). The column was washed with buffer B and the target protein was recovered in the flow-through fraction. The relevant fractions were pooled and loaded on a RESOURCE PHE column (GE Healthcare Biosciences; Piscataway, NJ, USA) and then eluted with a linear gradient of ammonium sulfate from 2 to 0 M using an ÄKTA system (GE Healthcare Biosciences). The fractions eluted from about 1.5 to 1.0 M ammonium sulfate were collected and concentrated using a Vivaspin 20 concentrator (3 kDa molecular-mass cutoff). The concentrated solution was applied on a Superdex 75 HR 10/300 column (GE Healthcare Biosciences) equilibrated with 50 mM Tris-HCl and 100 mM KCl, pH 8.0 using an ÄKTA system. Purified proteins, ttCSP1 and ttCSP2, were identified by the peptide mass finger printing method. ttCSP1 was prepared as described previously (published elsewhere).

9. CD measurements

The CD spectrum of 5 μM ttCSP1 or ttCSP2 was measured in the buffer containing 50 mM potassium phosphate and 100 mM KCl at pH 7.4 by using Jasco J720W spectropolarimeter (Japan Spectroscopic, Tokyo, Japan). Thermostability was measured in the range of temperature from 25 to 95°C at 216 nm by using a quartz cuvette with a path length of 0.1 cm. The rate of temperature change was 1°C/min.

10. Analytical size-exclusion chromatography

Analytical size-exclusion chromatography was performed to investigate the oligomer structure of ttCSP1 and ttCSP2 in the absence or presence of nucleic acid ligands by using Superdex 75 10/300 GL column (GE healthcare). The column was equilibrated in 20 mM

Tris-HCl (pH 8.0) and 200 mM NaCl. Elution of the protein was detected by UV absorbance (A_{280} and A_{260}). The sample solutions containing the proteins (47 μM) and dT7 (47 μM) or dT31 (8 μM) were prepared in 20 mM Tris-HCl (pH 8.0) and 200 mM NaCl. These solutions were incubated at room temperature for 5 min before measurement.

11. Fluorescence quenching assay.

Fluorescence intensities of ttCSP1 and ttCSP2 were measured by using F-4500 fluorescence spectrophotometer (HITACHI, Tokyo, Japan) with 5 × 5-mm cell at 25°C with excitation and emission wavelengths of 292 and 349 nm, respectively. The 0.5 μM ttCSP1 or ttCSP2 solution containing 25 mM Tris-HCl, 100 mM KCl, and 0.5 mM EDTA, pH 7.5, was successively titrated with ssDNA or ssRNA. The nucleotide sequences of ssDNA and ssRNA used in this experiment are shown in Table 4. LoopdT7, loopdT7dA4, loopdT11, stem5dT7 and stem3dT7 were prepared by incubating at 95°C for 2 min and 60°C for 10 min to form secondary structure as shown in Fig. 4.

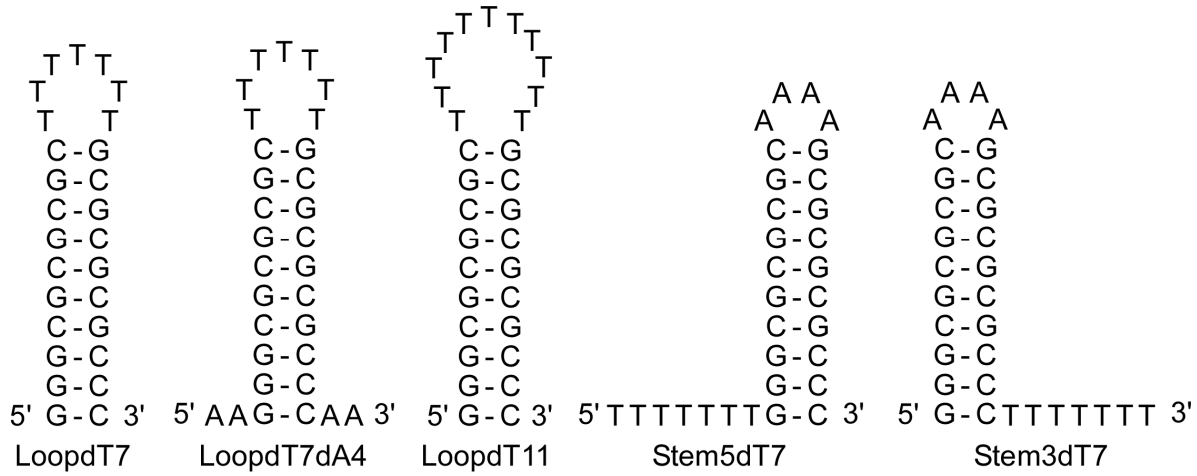

Fig. 4. The sequences and predicted secondary structures of loopdT7, loopdT7dA4, loopdT11, stem5dT7 and stem3dT7.

Table 4. The sequences of ssDNA and ssRNA ligands for binding assay.

Name	Nucleotide sequence	Length (bases)
dT3	TTT	3
dT4	TTTT	4
dT5	TTTTT	5
dT6	TTTTTT	6
dT7	TTTTTTT	7
dT8	TTTTTTTT	8
dT10	TTTTTTTTTT	10
dA7	AAAAAAA	7
dA31	AAAAAAAAAAAAAAAAAAAAAAAAAAAAAAA	31
dC7	CCCCCCC	7
dC31	CCCCCCCCCCCCCCCCCCCCCCCCCCCCCCC	31
dG7	GGGGGGG	7
dG31	GGGGGGGGGGGGGGGGGGGGGGGGGGGGGGG	31
LoopdT7	CCGGGCGCGCGCTTTTTTTGCGCGCGCCCGG	31
LoopdT7dA4	AACCGGGCGCGCGCTTTTTTTGCGCGCGCCCGGAA	35
LoopdT11	GGGCGCGCGCTTTTTTTTTTTGCGCGCGCCC	31
Stem5dT7	TTTTTTTGGGCGCGCGCAAAAGCGCGCGCCC	31
Stem3dT7	GGGCGCGCGCAAAAGCGCGCGCCCTTTTTTT	31
U7	UUUUUUU	7
21f	ATGACAACTAAACGAACACCC	21
21r	GGGTGTTGCTTTACTTGTCAT	21

The equilibrium dissociation constant, K_d, was determined as follows. The fluorescence quenching was analyzed assuming the following scheme for the interaction of CSP (P) with ssDNA or ssRNA ligand (L),

$$P + L \underset{}{\overset{K_d}{\rightleftharpoons}} PL \qquad (1)$$

where K_d is defined by

$$K_d = [P][L]/[PL] \qquad (2)$$

The parentheses denote concentration. The total concentrations of these proteins ($[P]_0$) and

ssDNA or ssRNA ligand ($[L]_0$) are related to the respective free concentrations ([P] and [L]) as follows:

$$[P]_0 = [P] + [PL] \quad (3)$$

$$[L]_0 = [L] + [PL] \quad (4)$$

The concentration of free ligand is obtained from Eqs. 2 to 4 (Eftink, 1997),

$$[L] = ([L]_0-[P]_0-K_d+\sqrt{([L]_0-[P]_0-K_d)^2+4\,K_d[L]_0})/2 \quad (5)$$

The apparent molar fluorescence intensity (F_{app}) is expressed as (Lohman and Bujalowski, 1991)

$$F_{app}\,[P]_0 = F_p\,[P] + F_{PL}\,[PL]$$

$$F_{app} = F_p + (F_{PL} - F_p)\,[L] / ([L] + K_d) \quad (6)$$

where F_P and F_{PL} are the molar fluorescence intensities of the protein and the protein-ligand complex, respectively. The three parameters, F_P, F_{PL}, and K_d were determined by fitting Eqs. 5 and 6 to the observed fluorescence intensities at various values of $[L]_0$ and $[P]_0$ and using a least square program for nonlinear functions.

12. Electrophoretic mobility shift assay

Electrophoretic mobility shift assay (EMSA) was performed to investigate the ability of ttCSP1 and ttCSP2 to bind to double-stranded DNA (dsDNA). The nucleotide sequences of 21f and 21r used in this experiment are shown in Table 4. The 21r was radiolabeled at the 5'-end with [γ-^{32}P]ATP using T4 polynucleotide kinase (TAKARA, Shiga, Japan). Two-fold amount of 21f was added to the 5'-^{32}P-labeled or unlabeled 21r. Then, these ssDNAs were annealed over night after heat-treatment at 95˚C for 2 min in the presence of 0.1 M KCl. The substrate radiolabeled and cold 21f-21r dsDNA were obtained by the above process. The reaction mixture, which contains 40 mM Tris-HCl (pH 7.5), 200 mM KCl, 2 mM EDTA,

10 nM radiolabeled dsDNA, 1 μM cold 21f-21r dsDNA and various concentration of ttCSP1 or ttCSP2, was incubated at 25˚C for 5 min. These samples were mixed with a native PAGE loading dye (8.3 mM Tris-HCl (pH 7.5), 17 mM KCl, 5% glycerol, 0.033% BPB and xylene cyanol). Then, these mixtures were loaded onto a 7.5% polyacrylamide gel and electrophoresed in 1 × TBE buffer. The gel was dried and placed in contact with an imaging plate. The bands were visualized and analyzed using a BAS2500 image analyzer.

Results and Discussion

1. Cold shock response of *T. thermophilus* HB8

First, I investigated the effects of the temperature downshift (from 70°C to 45°C) on the transcriptional level in *T. thermophilus* HB8 wild-type strain. The samples were prepared at 30 s and 10 min after the temperature downshift. Comparison of the microarray data identified the 33 and 55 genes that were up- and down-regulated, respectively, even at 30 s (Table 5). To our knowledge, such a rapid response to cold shock has not been reported previously. The particularly noteworthy among the up-regulated genes was the expression of *ttha0359* (*ttcsp2*), one of two cold shock protein homologues of *T. thermophilus* HB8. Expression of *ttcsp2* was up-regulated 44-fold. No other gene displayed such a dramatic increase in expression 30 s after cold shock. The second largest change was 5.80-fold for *ttha1499*, MoxR-related protein. The other genes that were up-regulated over 4-fold were *ttha0969* (4.02), *ttha0970* (4.52) and *ttha0972* (4.35), *ttha1141* (4.84), *ttha1448* (4.01) and *ttha1498* (5.00). It should be mentioned here that *ttha1498* encodes elongation factor G (EF-G-2). These may be involved in transcription of some of the genes which were induced or repressed after the rapid response to cold shock.

Among the down-regulated genes at 30 s, the largest fold-changes were observed for *tthb070* (survival protein SurE) and *tthb071* (a hypothetical protein), which showed 0.07-fold increased, that is, 14.3-fold decrease. SurE is a metal ion-dependent phosphatase specific to nucleoside monophosphate and is known to improve bacterial viability during stress conditions (Mura et al., 2003). The down-regulated genes included three transcriptional regulators: *ttha0145* (PhoB), *ttha0733* (MarR family) and *ttha1580* (GntR family). These may be involved in transcription of some of the genes which were induced or repressed after

the rapid response to cold shock.

Table 5. Subset of genes up- and down-regulated in *T. thermophilus* HB8 at 30 s after cold shock. ORFs with a *q* value ≤ 0.05 and a fold change of ≥2-fold relative to those before cold shock have been listed.

Locus tag	Fold	Annotation	*q* value	COG code		
TTHA0044	0.38	putative Na(+)/H(+) antiporter	0.0080	P		
TTHA0045	0.48	probable potassium uptake protein TrkA	0.0100	P	S	
TTHA0122	0.23	manganese-containing pseudocatalase	0.0176	P		
TTHA0144	0.35	sensor histidine kinase	0.0113	T		
TTHA0145	0.33	phosphate regulon transcriptional regulatory protein PhoB	0.0006	T	K	
TTHA0259	0.43	phosphate ABC transporter, periplasmid phosphate-biniding protein	0.0240	P		
TTHA0260	0.16	probable phosphate ABC transporter, permease protein	0.0089	P		
TTHA0261	0.19	probable phosphate ABC transporter, permease protein	0.0033	P		
TTHA0262	0.30	probable phosphate ABC transporter, ATP-binding protein	0.0022	P		
TTHA0303	2.01	hypothetical protein	0.0263	-		
TTHA0312	0.41	cytochrome caa3 oxidase subunit I (polypeptide I + III)	0.0345	C		
TTHA0359	44.49	cold shock protein	0.0083	K		
TTHA0364	0.50	type IV pilus assembly protein PilF	0.0468	N	U	
TTHA0470	0.43	peptide ABC transporter, permease protein	0.0184	E	P	
TTHA0471	0.39	peptide ABC transporter, permease protein	0.0239	E	P	
TTHA0485	0.44	phosphoesterase-related protein	0.0137	T		
TTHA0539	0.36	hypothetical protein	0.0065	R		
TTHA0605	0.45	4-hydroxybenzoate octaprenyltransferase	0.0085	H		
TTHA0607	2.25	biotin synthase (biotin synthetase)	0.0494	H		
TTHA0622	0.35	transcription elongation factor GreA	0.0269	K		
TTHA0706	2.77	cation-transporting ATPase	0.0230	P		
TTHA0727	3.27	hypothetical protein	0.0090	S		
TTHA0729	0.25	probable efflux transporter, AcrB/AcrD/AcrF family	0.0249	V		
TTHA0731	0.21	hypothetical protein	0.0077	M	U	
TTHA0732	0.23	hypothetical protein	0.0080	-		
TTHA0733	0.31	transcriptional regulator MarR family	0.0184	K		
TTHA0743	0.37	glycosyltransferase related protein	0.0264	M	N	U
TTHA0757	2.83	hypothetical protein	0.0168	-		
TTHA0759	0.28	homoserine O-acetyltransferase	0.0100	E		
TTHA0799	0.36	prephenate dehydrogenase	0.0242	E		
TTHA0800	0.38	phospho-2-dehydro-3-deoxyheptonate aldolase	0.0432	E		
TTHA0829	2.68	putative acetoin utilization protein, acetoin dehydrogenase	0.0044	R		
TTHA0957	0.27	dihydrodipicolinate synthase	0.0078	E	M	
TTHA0958	0.23	2-hydroxyhepta-2,4-diene-1,7-dioate isomerase/5-carboxymethyl-2-oxo-hex-3-ene-1,7-dioate decarboxylase	0.0153	Q		
TTHA0959	0.26	5-carboxymethyl-2-hydroxymuconate semialdehyde dehydrogenaseiheyensis HTE831]'	0.0203	C		
TTHA0968	2.64	phenylacetic acid degradation protein PaaZ	0.0475	C	I	
TTHA0969	4.02	phenylacetic acid degradation protein PaaD	0.0350	R		
TTHA0970	4.52	phenylacetic acid degradation protein PaaC	0.0339	S		
TTHA0971	3.87	phenylacetic acid degradation protein PaaB	0.0249	Q		
TTHA0972	4.35	phenylacetic acid degradation protein PaaA	0.0411	S		

TTHA0979	2.20	hypothetical protein	0.0165	G			
TTHA0980	2.21	hypothetical protein	0.0183	G			
TTHA1065	0.29	transcription termination factor Rho	0.0078	K			
TTHA1066	0.27	proabable transaldolase	0.0196	G			
TTHA1072	0.32	translation initiation factor, aIF-2B alpha subunit-related protein	0.0153	J			
TTHA1137	2.16	major facilitator superfamily transporter	0.0153	G	E	P	R
TTHA1141	4.84	cation-transporting ATPase	0.0008	P			
TTHA1172	0.43	alpha-glucan phosphorylase	0.0053	G			
TTHA1212	0.44	acetolactate synthase, small subunit (ilvN)	0.0190	E			
TTHA1222	0.26	pilin, type IV, putative	0.0083	-			
TTHA1317	2.08	immunogenic protein related protein	0.0152	R			
TTHA1325	0.45	putaitve sulfite oxidase	0.0416	R			
TTHA1326	0.38	cytochrome c-552 like protein	0.0427	C			
TTHA1327	0.45	hypothetical protein	0.0416	S			
TTHA1391	0.36	GTP-binding protein	0.0207	R			
TTHA1407	2.32	cytochrome c-type biogenesis protein, heme exporter protein B	0.0106	O			
TTHA1408	3.21	ABC transporter, ATP-binding protein	0.0008	V			
TTHA1447	3.01	alanine dehydrogenase	0.0056	E			
TTHA1448	4.01	4-hydroxybutyrate CoA-transferase	0.0079	C			
TTHA1498	5.00	elongation factor G (EF-G-2)	0.0044	J			
TTHA1499	5.80	MoxR-related protein	0.0053	R			
TTHA1500	2.12	phosphoenolpyruvate synthase	0.0190	G			
TTHA1570	0.37	deoxyhypusine synthase	0.0209	O			
TTHA1578	0.44	1-pyrroline-5-carboxylate dehydrogenase	0.0346	C			
TTHA1579	0.28	putative proline dehydrogenase (monofunctional)	0.0055	E			
TTHA1580	0.25	transcriptional regulator, GntR family	0.0065	K			
TTHA1626	2.87	hypothetical protein	0.0078	S			
TTHA1645	0.50	MutS2 protein	0.0285	L			
TTHA1696	0.46	30S ribosomal protein S7	0.0221	J			
TTHA1697	0.48	30S ribosomal protein S12	0.0274	J			
TTHA1724	0.48	hypothetical protein	0.0294	-			
TTHA1725	0.43	hypothetical protein	0.0044	-			
TTHA1784	2.14	putative preprotein translocase, SecG subunit	0.0288	U			
TTHA1891	2.01	hypothetical protein	0.0320	C			
TTHA1955	2.71	2-oxoacid--ferredoxin oxidoreductase, alpha chain	0.0207	C			
TTHA1956	2.35	2-oxoacid-ferredoxin oxidoreductase (EC 1.2.7.-) beta chain	0.0203	C			
TTHA1962	0.49	6-phosphofructokinase	0.0044	G			
TTHA1963	0.44	tetrapyrrole methylase family protein	0.0065	R			
TTHA1967	2.03	competence protein ComEA-related protein	0.0311	L			
TTHB024	0.48	hypothetical protein	0.0078	-			
TTHB067	0.14	alkaline phosphatase	0.0022	P			
TTHB070	0.07	survival protein SurE	0.0044	R			
TTHB071	0.06	hypothetical protein	0.0067	G			
TTHB156	0.47	hypothetical protein	0.0476	-			
TTHB158	0.43	hypothetical protein	0.0300	-			
TTHB185	2.84	hypothetical protein	0.0274	L			
TTHB187	2.66	hypothetical protein	0.0200	R			
TTHB188	2.05	comserved hypothetical protein	0.0086	-			

At 10 min after temperature downshift, 440 genes were found to be up- and down-regulated. The number of affected genes at 10 min was much larger than that at 30 s. However, it was not surprising that such a large number of genes were affected by temperature downshift: the expression of hundreds of genes involved in various cellular processes has been known to be affected.

171 genes were up-regulated (Table 6), some of which have been well known as CIPs. The *ttha0109* (10-fold increase) encodes an ATP-dependent RNA helicase, which is similar to the cold-induced DEAD box RNA helicase, *E. coli* CsdA (and also RhlE) and *B. subtilis* CshA and CshB (Hunger et al., 2006). The cold-induced DEAD box RNA helicase has been proposed to act as RNA chaperone in conjunction with CSPs (Hunger et al., 2006). The *ttha0948* (12-fold increase) encodes fatty acid desaturase, whose homologue is cold-induced in *B. subtilis* (Aguilar et al., 1998). Fatty acid desaturase is thought to regulate membrane fluidity by introducing a cis-double bond at the fifth position of the acyl chain of membrane phospholipids. Expression of these genes barely changed 30 s after cold shock, suggesting that they were induced after the rapid cold shock response.

Of the 269 down-regulated genes (Table 6), some gene clusters encoding ribosomal proteins (*ttha1663–1697*, *ttha0209–0210*, and *ttha0242–0247*), ATP synthase subunits (*ttha1274–1277*) and NADH-quinone oxidoreductase subunits (*ttha0084–0097*) were identified. These are involved in protein synthesis and oxidative phosphorylation required for cell growth. Similar transcriptional changes of ATP synthase subunits were reported for other bacteria under the cold stress condition (Beckering et al., 2002). These results suggest that cold adaptation mechanisms of *T. themophilus* HB8 are akin to those of other bacteria.

Table 6. Subset of genes up- and down-regulated in *T. thermophilus* HB8 at 10 min after cold shock. ORFs with a *q* value ≤ 0.05 and a fold change of ≥2-fold relative to those before cold shock have been listed.

Locus tag	Fold	Annotation	*q* value	COG code
TTHA0003	0.43	pyruvate kinase	0.0029	G
TTHA0019	0.43	hypothetical protein	0.0114	S
TTHA0024	3.09	penicillin acylase II precursor	0.0024	R
TTHA0028	4.64	putative macrolide-efflux protein	0.0030	G E P R
TTHA0049	2.05	diacylglycerol kinase-related protein	0.0104	I R
TTHA0062	0.38	alanine racemase	0.0030	M
TTHA0066	0.39	hypothetical protein	0.0042	-
TTHA0072	2.35	hypothetical protein	0.0130	V
TTHA0079	2.34	hypothetical protein	0.0079	-
TTHA0084	0.14	NADH-quinone oxidoreductase chain 7	0.0010	C
TTHA0085	0.19	NADH-quinone oxidoreductase chain 6	0.0041	C
TTHA0086	0.24	NADH-quinone oxidoreductase chain 5	0.0014	C
TTHA0087	0.36	NADH-quinone oxidoreductase chain 4	0.0010	C
TTHA0088	0.46	NADH-quinone oxidoreductase chain 2	0.0027	C
TTHA0089	0.46	NADH-quinone oxidoreductase chain 1	0.0010	C
TTHA0090	0.49	NADH-quinone oxidoreductase chain 3	0.0227	C
TTHA0093	0.48	NADH-quinone oxidoreductase chain 10	0.0069	-
TTHA0096	0.44	NADH-quinone oxidoreductase chain 13	0.0223	C
TTHA0097	0.49	NADH-quinone oxidoreductase chain 14	0.0071	C
TTHA0109	10.14	ATP-dependent RNA helicase	0.0083	L K J
TTHA0111	5.51	hypothetical protein	0.0020	G E P R
TTHA0112	2.34	endonuclease III	0.0072	L
TTHA0120	4.77	GTP-binding protein Era	0.0094	R
TTHA0124	0.49	branched-chain amino acid aminotransferase (IlvE)	0.0130	E H
TTHA0127	2.87	tRNA (guanosine-2'-O-) methyltransferase	0.0028	J
TTHA0128	2.89	ATP phosphoribosyltransferase	0.0022	E
TTHA0130	2.67	deoxycytidine triphosphate deaminase	0.0071	F
TTHA0144	2.74	sensor histidine kinase	0.0250	T
TTHA0145	3.08	phosphate regulon transcriptional regulatory protein PhoB	0.0010	T K
TTHA0148	0.48	ribosomal large subunit pseudouridine synthase B	0.0026	J
TTHA0152	0.41	tungsten-containing aldehyde:ferredoxin oxidoreductase	0.0149	C
TTHA0153	0.35	NADPH:quinone reductase	0.0048	C R
TTHA0158	3.36	alpha-dextran endo-1,6-alpha-glucosidase ((amylo)pullulanase)	0.0022	G
TTHA0177	0.40	ferredoxin	0.0127	C
TTHA0179	0.50	hypothetical protein	0.0051	H
TTHA0184	0.45	pyruvate dehydrogenase complex, dihydrolipoamide acetyltransferase E2 component	0.0028	C
TTHA0185	0.41	pyruvate dehydrogenase complex, pyruvate dehydrogenase E1 component	0.0010	C
TTHA0192	0.35	hypothetical protein	0.0012	T
TTHA0196	0.38	transporter, periplasmic component	0.0155	Q
TTHA0200	0.49	molybdopterin oxidoreductase	0.0022	C
TTHA0201	0.42	Mg(2+) chelatase family protein	0.0076	O
TTHA0202	0.48	hypothetical protein	0.0026	S
TTHA0206	0.24	nicotinamide nucleotide transhydrogenase, alpha subunit 1	0.0158	C
TTHA0207	0.26	nicotinamide nucleotide transhydrogenase, alpha subunit 2	0.0030	C
TTHA0208	0.34	nicotinamide nucleotide transhydrogenase, beta subunit	0.0031	C

TTHA0211	2.46	lipoprotein releasing system transmembrane protein	0.0023	M			
TTHA0212	7.02	hypothetical protein	0.0019	S			
TTHA0230	0.37	2-oxoisovalerate dehydrogenase, E1 component beta subunit	0.0065	C			
TTHA0231	0.35	2-oxoisovalerate dehydrogenase, E1 component beta subunit	0.0015	-			
TTHA0232	0.37	pyruvate dehydrogenase complex, dihydrolipoamide acetyltranferase E2 component	0.0048	C			
TTHA0242	0.48	50S ribosomal protein L9	0.0029	J			
TTHA0253	2.05	hypothetical protein	0.0031	-			
TTHA0255	0.27	ferric uptake regulation protein	0.0024	P			
TTHA0260	4.05	probable phosphate ABC transporter, permease protein	0.0075	P			
TTHA0261	2.40	probable phosphate ABC transporter, permease protein	0.0030	P			
TTHA0283	0.45	argininosuccinate lyase	0.0478	E			
TTHA0284	0.45	argininosuccinate synthetase	0.0313	E			
TTHA0285	0.47	hypothetical protein	0.0229	-			
TTHA0287	0.40	2-oxoglutarate dehydrogenase E3 component (dihydrolipoamide dehydrogenase)	0.0075	C			
TTHA0296	2.30	RNA methyltransferase, TrmH family	0.0079	J			
TTHA0306	3.05	queuine tRNA ribosyltransferase	0.0022	J			
TTHA0308	2.37	uracil permease [C-terminal]	0.0067	F			
TTHA0310	0.48	cytochrome c oxidase assembly factor (CtaA) + protoheme IX farnesyltransferase (CtaB)	0.0079	O			
TTHA0313	0.40	hypothetical protein	0.0040	I			
TTHA0316	0.39	hypothetical protein	0.0030	-			
TTHA0320	2.80	methionyl-tRNA formyltransferase	0.0031	J			
TTHA0321	2.62	polypeptide deformylase	0.0024	J			
TTHA0328	0.38	probable isochorismatase	0.0178	Q			
TTHA0338	0.42	hypothetical protein	0.0179	S			
TTHA0339	0.46	hypothetical protein	0.0098	R			
TTHA0345	2.01	porphobilinogen deaminase	0.0051	H			
TTHA0351	2.82	probable efflux protein (fosmidomycin resistance)	0.0023	G	E	P	R
TTHA0354	0.41	ABC transporter, permease protein, MalFG family	0.0011	G			
TTHA0355	0.28	ABC transporter, permease protein, MalFG family	0.0045	G			
TTHA0356	0.24	ABC transporter, periplasmic substrate-binding protein	0.0016	G			
TTHA0377	8.38	sugar ABC transporter, permease protein	0.0010	G			
TTHA0391	3.84	hypothetical protein	0.0057	R			
TTHA0399	0.27	hypothetical protein	0.0233	-			
TTHA0405	3.15	hypothetical protein	0.0024	T			
TTHA0408	3.41	ribosomal large subunit pseudouridine synthase D	0.0043	J			
TTHA0409	4.82	putative modification methylase	0.0024	L			
TTHA0410	4.80	hypothetical protein	0.0012	-			
TTHA0422	3.35	UDP-N-acetyl-D-mannosaminuronic acid transferase	0.0029	M			
TTHA0423	2.33	hypothetical protein	0.0024	-			
TTHA0435	2.82	disulfide bond formation protein B	0.0076	O			
TTHA0451	0.22	probable branched-chain amino acid ABC transporter, amno acid binding protein	0.0032	E			
TTHA0452	0.36	branched-chain amino acid ABC transporter, ATP-binding protein	0.0271	E			
TTHA0455	0.50	rrf2 family protein, transcriptional regulator	0.0029	K			
TTHA0462	0.42	hypothetical protein	0.0068	-			
TTHA0465	0.23	thioredoxin reductase	0.0030	O			
TTHA0466	0.20	alcohol dehydrogenase	0.0043	C	R		
TTHA0470	2.94	peptide ABC transporter, permease protein	0.0022	E	P		
TTHA0471	2.16	peptide ABC transporter, permease protein	0.0229	E	P		
TTHA0477	2.55	probable ATP pyrophosphatase, PP-loop superfamily	0.0046	D			

TTHA0484	0.35	apolipoprotein N-acyltransferase	0.0027	M			
TTHA0488	0.35	antitoxin of toxin-antitoxin stability system	0.0028	D			
TTHA0497	8.45	oxygen-independent coproporphyrinogen III oxidase	0.0010	H			
TTHA0498	3.91	hypothetical protein	0.0079	-			
TTHA0504	0.39	glycolate oxidase subunit GlcE	0.0051	C			
TTHA0505	0.31	glycolate oxidase subunit	0.0022	C			
TTHA0506	0.27	malate synthase	0.0046	C			
TTHA0507	0.37	transcriptional regulator	0.0145	K			
TTHA0508	0.43	transcriptional regulator, MerR family	0.0221	K			
TTHA0510	0.42	CsaA protein	0.0025	R			
TTHA0516	0.50	hypothetical protein	0.0071	-			
TTHA0525	0.45	glycine dehydrogenase (decarboxylating) subunit 1	0.0155	E			
TTHA0526	0.45	glycine dehydrogenase subunit 2 (P-protein)	0.0028	E			
TTHA0534	0.24	aspartokinase (aspartate kinase) [contains: aspartokinase alpha subunit; aspartokinase beta subunit]	0.0023	E			
TTHA0535	0.39	purine phosphoribosyltransferase (xanthine-guanine phosphoribosyltransferase)	0.0091	R			
TTHA0536	0.41	malate dehydrogenase	0.0075	C			
TTHA0538	0.50	succinyl-CoA synthetase beta chain	0.0098	C			
TTHA0548	0.48	hypothetical protein	0.0026	-			
TTHA0554	2.61	small multidrug export protein	0.0171	S			
TTHA0557	0.38	superoxide dismutase [Mn]	0.0022	P			
TTHA0566	3.33	GTP-binding protein HflX	0.0032	R			
TTHA0583	0.40	hypothetical protein	0.0020	S			
TTHA0585	0.43	branched-chain amino acid ABC transporter, permease protein	0.0041	E			
TTHA0586	0.44	putative long-chain-fatty-acid--CoA ligase	0.0183	I			
TTHA0588	0.41	branched-chain amino acid ABC transport ATP-binding protein	0.0293	E			
TTHA0589	0.39	branched-chain amino acid ABC transporter permease protein	0.0081	E			
TTHA0590	0.33	branched-chain amino acid ABC transporter amino acid-binding protein	0.0030	E			
TTHA0595	0.48	galactokinase	0.0409	G			
TTHA0602	2.69	peptidyl-prolyl cis-trans isomerase	0.0030	O			
TTHA0605	2.82	4-hydroxybenzoate octaprenyltransferase	0.0012	H			
TTHA0608	2.96	probable RNA-biniding protein	0.0048	K			
TTHA0618	2.66	5-methyltetrahydrofolate homocysteine S-methyltransferase	0.0038	E			
TTHA0620	0.29	alternative anthranilate synthase component I+II (TrpEG)	0.0042	E	H		
TTHA0623	0.44	DNA repair protein RecO	0.0209	-			
TTHA0630	2.98	heat shock protein HslU	0.0060	O			
TTHA0631	2.55	heat shock protein HslV	0.0089	O			
TTHA0649	2.91	putative O-antigen transporter	0.0028	R			
TTHA0672	2.12	probable sulfite reductase	0.0133	P			
TTHA0679	0.42	putative transport protein	0.0038	G	E	P	R
TTHA0681	0.14	hypothetical protein	0.0022	-			
TTHA0682	0.21	hypothetical protein	0.0031	-			
TTHA0697	0.31	probable SecDF protein-export membrane protein	0.0017	U			
TTHA0698	0.45	hypothetical protein	0.0127	-			
TTHA0713	0.42	hypothetical protein	0.0030	-			
TTHA0718	0.42	uracil-DNA glycosylase	0.0031	L			
TTHA0719	0.40	hypothetical protein	0.0083	-			
TTHA0724	2.21	serine protease	0.0139	O			
TTHA0725	6.33	membrane-bound protein LytR	0.0029	K			
TTHA0726	0.47	aconitate hydratase (aconitase)	0.0079	C			
TTHA0727	0.36	hypothetical protein	0.0057	S			

TTHA0731	4.49	hypothetical protein	0.0031	M	U	
TTHA0732	6.27	hypothetical protein	0.0014	-		
TTHA0733	4.19	transcriptional regulator MarR family	0.0041	K		
TTHA0740	2.17	sensor histidine kinase	0.0083	T		
TTHA0741	2.60	GTP-binding elongation factor family LepA	0.0038	M		
TTHA0743	20.22	glycosyltransferase related protein	0.0022	M	N	U
TTHA0744	13.28	hypothetical protein	0.0017	O		
TTHA0745	2.93	hypothetical protein	0.0199	-		
TTHA0746	0.34	iron ABC transporter, substrate-binding protein	0.0030	P		
TTHA0747	0.26	iron ABC transporter, permease protein	0.0026	P		
TTHA0748	0.35	iron ABC transporter, ATP-binding protein	0.0030	P	H	
TTHA0749	0.41	hypothetical protein	0.0079	-		
TTHA0750	0.40	3-oxoacyl-[acyl carrier protein] reductase	0.0022	I	Q	R
TTHA0754	0.47	transcriptional repressor	0.0031	K		
TTHA0760	3.79	O-acetyl-L-homoserine sulfhydrylase	0.0045	E		
TTHA0763	0.40	zinc-dependent dehydrogenase	0.0148	E	R	
TTHA0764	0.49	hypothetical protein	0.0300	G		
TTHA0765	0.46	probable hydrolase	0.0012	E	Q	
TTHA0766	0.42	ABC transporter, solute-binding protein	0.0153	Q		
TTHA0767	0.42	putative small integral membrane tranport protein	0.0029	Q		
TTHA0769	2.41	periplasmic serine protease, HtrA/DegQ/DegS family	0.0063	O		
TTHA0781	0.47	dihydroorotase (PyrC)	0.0119	F		
TTHA0784	2.64	hypothetical protein	0.0011	-		
TTHA0785	3.69	hypothetical protein	0.0023	R		
TTHA0786	5.22	glycerate dehydrogenase/glyoxylate reductase	0.0029	C	H	R
TTHA0790	0.47	putative acetyltransferase	0.0117	K	R	
TTHA0799	4.96	prephenate dehydrogenase	0.0030	E		
TTHA0800	4.64	phospho-2-dehydro-3-deoxyheptonate aldolase	0.0053	E		
TTHA0801	5.73	hypothetical protein	0.0041	R		
TTHA0802	3.59	hypothetical protein	0.0020	S		
TTHA0803	2.14	hypothetical protein	0.0023	R		
TTHA0805	4.68	hypothetical protein	0.0021	-		
TTHA0825	2.29	S-adenosylmethionine decarboxylase proenzyme	0.0106	E		
TTHA0829	0.36	putative acetoin utilization protein, acetoin dehydrogenase	0.0040	R		
TTHA0843	2.14	serine protein kinase	0.0494	T		
TTHA0844	2.44	CAAX amino terminal protease family protein	0.0030	-		
TTHA0856	0.44	1-deoxy-D-xylulose-5-phosphate reductoisomerase	0.0045	I		
TTHA0857	0.28	phosphatidate cytidylyltransferase	0.0039	I		
TTHA0867	0.31	hypothetical protein	0.0041	-		
TTHA0888	2.83	pyrrolidone carboxyl peptidase	0.0061	O		
TTHA0889	2.56	transcription-repair coupling factor	0.0022	L	K	
TTHA0898	0.30	hypothetical protein	0.0364	R		
TTHA0903	0.24	probable hydrolase	0.0064	R		
TTHA0904	0.26	biotin biosynthesis protein BioY	0.0060	R		
TTHA0905	0.31	glyceraldehyde 3-phosphate dehydrogenase (GAPDH)	0.0012	G		
TTHA0906	0.35	phosphoglycerate kinase	0.0045	G		
TTHA0928	2.20	methyltransferase	0.0219	L		
TTHA0931	3.29	thiophene and furan oxidation protein	0.0042	R		
TTHA0945	2.99	hypothetical protein	0.0164	-		
TTHA0947	6.03	triosephosphate isomerase	0.0035	G		
TTHA0948	12.28	fatty acid desaturase	0.0137	I		

TTHA0953	2.52	hypothetical protein	0.0447	K	
TTHA0954	2.07	mannosyl-3-phosphoglycerate synthase	0.0149	-	
TTHA0956	2.21	hypothetical protein	0.0073	T	Q
TTHA0957	2.88	dihydrodipicolinate synthase	0.0041	E	M
TTHA0958	2.30	2-hydroxyhepta-2,4-diene-1,7-dioate isomerase/5-carboxymethyl-2-oxo-hex-3-ene-1,7-dioate decarboxylase	0.0171	Q	
TTHA0962	0.41	homoprotocatechuate 2,3-dioxygenase	0.0432	E	
TTHA0963	0.26	ABC tranpsorter ATP binding protein related protein	0.0180	E	
TTHA0964	0.27	ABC tranpsorter ATP binding protein related protein	0.0406	E	
TTHA0965	0.32	phenylacetic acid degradation protein PaaI	0.0098	Q	
TTHA0966	0.24	phenylacetyl-CoA ligase	0.0303	H	
TTHA0967	0.33	hypothetical protein	0.0476	R	
TTHA0979	0.16	hypothetical protein	0.0020	G	
TTHA0980	0.15	hypothetical protein	0.0012	G	
TTHA0981	0.35	hypothetical protein	0.0068	K	
TTHA0987	0.41	beta-ketoadipyl CoA thiolase	0.0173	I	
TTHA0999	0.43	hypothetical protein	0.0178	T	
TTHA1003	2.69	sensor histidine kinase	0.0016	T	
TTHA1009	0.35	hypothetical protein	0.0042	K	
TTHA1010	0.33	hypothetical protein	0.0015	V	
TTHA1028	0.27	thiosulfate sulfurtransferase	0.0032	P	
TTHA1029	2.37	L-serine dehydratase, alpha subunit	0.0044	E	
TTHA1038	0.43	methylmalonyl-CoA mutase, alpha subunit, chain B	0.0030	I	
TTHA1039	0.25	methylmalonyl-CoA mutase, alpha subunit, chain A	0.0064	I	
TTHA1050	0.46	shikimate 5-dehydrogenase	0.0094	E	
TTHA1060	0.46	Mg2+ transporter MgtE	0.0081	P	
TTHA1062	0.32	GTP cyclohydrolase II/3,4-dihydroxy-2-butanone-4-phosphate synthase	0.0045	H	
TTHA1063	0.35	riboflavin synthase alpha chain	0.0024	H	
TTHA1066	2.51	proabable transaldolase	0.0146	G	
TTHA1070	2.00	hypothetical protein	0.0057	M	
TTHA1078	0.42	penicillin-binding protein	0.0149	M	
TTHA1079	0.37	UDP-N-acetylmuramoylalanyl-D-glutamyl-2,6-diaminopimelate--D-alanyl-D-alanyl ligase	0.0022	M	
TTHA1080	0.42	hypothetical protein	0.0030	-	
TTHA1082	0.45	UDP-N-acetylmuramoylalanine--D-glutamiate ligase	0.0022	M	
TTHA1091	0.41	hypothetical protein	0.0044	S	
TTHA1098	0.45	membrane lipoprotein	0.0242	R	
TTHA1110	2.51	hypothetical protein	0.0206	M	
TTHA1126	3.42	hypothetical protein	0.0030	-	
TTHA1134	0.25	ba3-type cytochrome c oxidase polypeptide II	0.0017	C	
TTHA1135	0.29	ba3-type cytochrome c oxidase polypeptide I	0.0064	C	
TTHA1145	0.30	electron transfer flavoprotein, beta subunit	0.0068	C	
TTHA1146	0.32	electron transfer flavoprotein, alpha subunit	0.0041	C	
TTHA1153	2.10	mercuric reductase	0.0091	C	
TTHA1172	3.31	alpha-glucan phosphorylase	0.0022	G	
TTHA1185	2.92	GTP-binding protein	0.0012	J	
TTHA1192	0.48	septum site-determining protein MinC	0.0080	D	
TTHA1203	2.12	hypothetical protein	0.0056	S	
TTHA1209	0.44	probable acetyltransferase	0.0045	K	R
TTHA1212	3.39	acetolactate synthase, small subunit (ilvN)	0.0071	E	
TTHA1213	3.44	acetolactate synthase, large subunit	0.0082	E	H
TTHA1234	0.36	dihydroxyacid dehydratase	0.0026	E	G

TTHA1236	0.47	spermidine/putrescine ABC transporter, periplasmic spermidine/putrescine-binding protein	0.0028	E		
TTHA1248	0.28	acetyl-coenzyme A synthetase	0.0083	I		
TTHA1255	0.46	hypothetical protein	0.0021	P		
TTHA1256	0.42	hypothetical protein	0.0053	S		
TTHA1261	2.85	4-alpha-glucanotransferase (amylomaltase) (disproportionating enzyme) (D-enzyme)	0.0076	G		
TTHA1268	2.31	hypothetical protein	0.0183	-		
TTHA1270	2.11	V-type ATP synthase, subunit (VTPJ-THERM)	0.0030	-		
TTHA1274	0.41	V-type ATP synthase subunit F	0.0023	C		
TTHA1275	0.36	V-type ATP synthase subunit	0.0029	C		
TTHA1276	0.42	V-type ATP synthase subunit E	0.0031	-		
TTHA1277	0.33	V-type ATP synthase, subunit K	0.0040	C		
TTHA1280	4.91	hypothetical protein	0.0017	R		
TTHA1283	0.43	hypothetical protein	0.0030	R		
TTHA1285	0.41	acetyl-coenzyme A synthetase	0.0063	I		
TTHA1288	0.45	exonuclease SbcC	0.0064	L		
TTHA1294	0.39	ribosomal subunit interface protein	0.0135	J		
TTHA1301	0.30	hypothetical protein	0.0010	R		
TTHA1306	2.73	hypothetical protein	0.0090	-		
TTHA1317	0.32	immunogenic protein related protein	0.0029	R		
TTHA1322	0.44	S-adenosylmethionine:2-demethylmenaquinone methyltransferase	0.0022	H		
TTHA1325	0.38	putaitve sulfite oxidase	0.0160	R		
TTHA1328	0.42	5'-nucleotidase precursor	0.0212	F		
TTHA1341	2.54	ABC transporter, ATP-binding protein	0.0056	V		
TTHA1342	2.35	ABC transporter, ATP-binding protein	0.0057	V		
TTHA1350	2.11	hypothetical protein	0.0142	L	K	J
TTHA1351	2.80	peptidase, M20/M25/M40 family	0.0083	E		
TTHA1367	0.44	hypothetical protein	0.0145	S		
TTHA1372	2.38	N-acetylmuramoyl-L-alanine amidase	0.0043	M		
TTHA1376	4.33	HD domain protein	0.0065	T		
TTHA1377	2.37	hypothetical protein	0.0030	-		
TTHA1385	2.19	shikimate kinase	0.0096	E		
TTHA1388	2.03	holo-[acyl carrier protein] synthase	0.0100	I		
TTHA1389	2.72	hypothetical protein	0.0029	S		
TTHA1391	4.54	GTP-binding protein	0.0029	R		
TTHA1393	0.45	hypothetical protein	0.0043	S	G	
TTHA1409	2.09	cytochrome c-type biogenesis protein CcdA	0.0023	O		
TTHA1412	0.24	sulfide dehydrogenase flavocytochrome C	0.0078	R		
TTHA1422	3.08	thioredoxin	0.0227	O	C	
TTHA1434	0.44	3-hydroxybutyryl-CoA dehydratase	0.0163	I		
TTHA1436	0.47	ABC-type transporter, ATP-binding protein	0.0010	V		
TTHA1439	0.47	probable sugar aminotransferase	0.0080	M		
TTHA1440	4.32	excinuclease ABC subunit A (UvrA)	0.0040	L		
TTHA1441	4.05	hypothetical protein	0.0113	S		
TTHA1442	2.32	glucose inhibited division protein	0.0145	J		
TTHA1447	0.39	alanine dehydrogenase	0.0028	E		
TTHA1457	0.45	S-adenosylmethionine decarboxylase proenzyme	0.0123	E		
TTHA1463	0.17	long-chain-fatty-acid--CoA ligase	0.0022	I	Q	
TTHA1487	0.41	ATP-dependent Clp protease, ATP-binding subunit ClpB	0.0104	O		
TTHA1488	0.47	DafA protein (DnaK-DnaJ assembly factor A)	0.0135	K		
TTHA1489	0.40	chaperone protein DnaJ	0.0057	O		

TTHA1498	0.23	elongation factor G (EF-G-2)	0.0069	J	
TTHA1499	0.34	MoxR-related protein	0.0080	R	
TTHA1502	2.46	response regulator	0.0094	T	K
TTHA1505	4.13	cytochrome c assembly protein-related protein	0.0033	O	
TTHA1518	0.43	2-haloalkanoic acid dehalogenase-related protein	0.0029	R	
TTHA1519	0.47	phosphoribosylformylglycinamidine synthase II	0.0051	F	
TTHA1530	0.34	hypothetical protein	0.0041	R	
TTHA1539	2.87	putative phage integrase/recombinase	0.0079	L	
TTHA1540	2.52	hypothetical protein	0.0156	-	
TTHA1563	2.05	(neo)pullulanase	0.0065	G	
TTHA1569	3.05	hypothetical protein	0.0154	Q	R
TTHA1570	2.91	deoxyhypusine synthase	0.0141	O	
TTHA1572	2.45	hypothetical protein	0.0030	R	
TTHA1582	0.42	2-amino-3-ketobutyrate CoA ligase (glycine acetyltransferase)	0.0051	H	
TTHA1591	0.48	hypothetical protein	0.0433	-	
TTHA1612	0.46	putative hydrolase	0.0060	R	
TTHA1619	2.16	probable methyltransferase	0.0081	R	
TTHA1621	0.38	heat shock protein, class I	0.0048	O	
TTHA1625	0.32	osmotically inducible protein OsmC	0.0024	O	
TTHA1626	0.19	hypothetical protein	0.0024	S	
TTHA1635	0.23	iron-sulfur cluster biosynthesis protein IscA	0.0027	S	
TTHA1641	6.24	GGDEF domain protein	0.0050	T	
TTHA1645	6.13	MutS2 protein	0.0012	L	
TTHA1653	3.71	hypothetical protein	0.0010	-	
TTHA1663	0.50	50S ribosomal protein L17	0.0395	J	
TTHA1664	0.42	DNA-directed RNA polymerase alpha chain	0.0075	K	
TTHA1665	0.46	30S ribosomal protein S4	0.0169	J	
TTHA1671	0.46	adenylate kinase	0.0252	F	
TTHA1705	2.54	probable esterase	0.0165	R	
TTHA1708	2.28	hypothetical protein	0.0022	I	
TTHA1710	2.20	radical SAM domain protein	0.0234	O	
TTHA1718	0.46	heavy metal binding protein	0.0366	P	
TTHA1724	2.12	hypothetical protein	0.0064	-	
TTHA1725	2.78	hypothetical protein	0.0060	-	
TTHA1726	3.19	S-layer repressor	0.0254	R	
TTHA1727	2.94	hypothetical protein	0.0301	-	
TTHA1728	4.23	hypothetical protein	0.0037	O	C
TTHA1743	5.07	orotidine 5'-phosphate decarboxylase	0.0020	F	
TTHA1748	2.14	hypothetical protein	0.0491	J	
TTHA1751	0.41	putative glycosyltransferase	0.0048	M	
TTHA1752	0.39	hypothetical protein	0.0095	-	
TTHA1759	0.48	hypothetical protein	0.0451	S	
TTHA1765	2.82	hypothetical protein	0.0124	-	
TTHA1767	2.42	acetyl-CoA carboxylase carboxyl transferase, alpha subunit (AccA)	0.0012	I	
TTHA1768	2.32	acetyl-CoA carboxylase carboxyl transferase, beta subunit (AccD)	0.0189	I	
TTHA1776	5.03	hypothetical protein	0.0044	-	
TTHA1795	2.66	MutT/nudix family protein	0.0158	F	
TTHA1813	2.31	DNA-directed RNA polymerase beta chain (RpoB)	0.0041	K	
TTHA1819	2.22	2'-5' RNA ligase	0.0065	J	
TTHA1822	3.86	probable transporter	0.0024	-	
TTHA1823	2.98	putative hydrolase (phosphatase)	0.0043	R	

TTHA1827	2.13	sugar ABC transporter permease protein	0.0080	G	
TTHA1848	0.27	hypothetical protein	0.0033	-	
TTHA1849	0.27	hypothetical protein	0.0051	-	
TTHA1850	0.21	hypothetical protein	0.0012	-	
TTHA1853	2.66	arsenate reductase	0.0061	T	
TTHA1855	2.09	ABC transporter, permease protein	0.0130	R	
TTHA1869	0.34	hypothetical protein	0.0069	-	
TTHA1882	2.70	hypothetical protein	0.0335	T	
TTHA1892	2.53	excinuclease ABC subunit B (UvrB)	0.0073	L	
TTHA1895	0.32	hypothetical protein	0.0081	-	
TTHA1903	0.45	putative acetylglutamate kinase	0.0029	E	
TTHA1917	0.38	3-octaprenyl-4-hydroxybenzoate carboxy-lyase	0.0040	H	
TTHA1923	2.17	sodium ABC transporter, permease protein NatB	0.0160	C	P
TTHA1924	2.26	sodium ABC transporter, ATP-binding protein NatA	0.0047	C	P
TTHA1931	0.45	quinol-cytochrome c reductase, Rieske iron-sulfur subunit	0.0022	C	
TTHA1941	0.44	ZIP zinc transporter family protein	0.0051	P	
TTHA1953	0.39	hypothetical protein	0.0202	S	
TTHA1955	0.40	2-oxoacid--ferredoxin oxidoreductase, alpha chain	0.0261	C	
TTHA1956	0.38	2-oxoacid-ferredoxin oxidoreductase (EC 1.2.7.-) beta chain	0.0119	C	
TTHA1959	0.40	phenylalanyl-tRNA synthetase beta chain	0.0132	J	R
TTHA1963	2.22	tetrapyrrole methylase family protein	0.0033	R	
TTHB002	2.39	hypothetical protein	0.0051	-	
TTHB006	0.41	hypothetical protein	0.0041	-	
TTHB007	0.27	hypothetical protein	0.0081	S	
TTHB010	2.24	transposase-related protein	0.0010	L	
TTHB018	0.40	hypothetical protein	0.0031	Q	
TTHB021	0.42	hypothetical protein	0.0048	V	
TTHB033	0.45	alpha-glucosidase	0.0267	G	
TTHB034	0.45	putative beta-mannosidase	0.0258	G	
TTHB037	0.43	hypothetical protein	0.0057	-	
TTHB046	2.25	cobalamin (5'-phosphate) synthase	0.0024	-	
TTHB049	0.45	alpha-ribazole-5'-phosphate phosphatase	0.0084	G	
TTHB050	0.15	probable high-affinity nickel permease	0.0023	P	
TTHB051	0.21	cobalamin biosynthetic protein	0.0043	H	
TTHB052	0.23	cobalamin biosynthesis precorrin-8X isomerase	0.0097	H	
TTHB053	0.26	precorrin-6Y C5,15-methyltransferase [decarboxylating]	0.0051	H	
TTHB054	0.39	precorrin-2 methylase	0.0283	H	
TTHB055	0.40	precorrin-4 C11-methyltransferase	0.0065	H	
TTHB056	0.38	precorrin-3 C17-methyltransferase	0.0151	H	
TTHB057	0.37	cobalamin biosynthesis protein CbiG	0.0023	H	
TTHB059	0.33	hypothetical protein	0.0022	-	
TTHB060	0.30	S-adenosyl-L-methionine uroporphyrinogen methyltransferase	0.0030	H	
TTHB061	0.43	cobalamin biosynthesis nitroreductase BluB	0.0023	C	
TTHB068	0.41	hypothetical protein	0.0102	J	
TTHB070	16.76	survival protein SurE	0.0017	R	
TTHB071	37.74	hypothetical protein	0.0020	G	
TTHB082	0.35	sugar ABC transporter, periplasmic sugar-binding protein	0.0032	G	
TTHB088	0.39	Zn-dependent hydrolase	0.0344	R	
TTHB094	0.50	putative short-chain oxidoreductase	0.0039	-	
TTHB116	0.40	acyl-CoA dehydrogenase, short-chain specific (probable AidB protein)	0.0028	I	
TTHB120	0.41	hypothetical protein	0.0126	-	

TTHB131	5.62	hypothetical protein	0.0022	-
TTHB142	0.50	glycerol kinase	0.0214	C
TTHB143	0.37	putative glycerol-3-phohsphate dehydrogenase	0.0113	C
TTHB144	0.41	hypothetical protein	0.0083	-
TTHB147	0.30	hypothetical protein	0.0010	R
TTHB148	0.33	hypothetical protein	0.0020	-
TTHB149	0.34	hypothetical protein	0.0037	L
TTHB150	0.25	hypothetical protein	0.0041	-
TTHB151	0.26	hypothetical protein	0.0030	L
TTHB152	0.22	hypothetical protein	0.0010	L
TTHB155	0.33	hypothetical protein	0.0042	-
TTHB160	0.30	hypothetical protein	0.0041	R
TTHB161	0.32	hypothetical protein	0.0081	L
TTHB162	0.38	hypothetical protein	0.0065	L
TTHB163	0.31	hypothetical protein	0.0046	L
TTHB164	0.26	hypothetical protein	0.0028	L
TTHB165	0.36	hypothetical protein	0.0078	L
TTHB166	2.21	hypothetical protein	0.0012	-
TTHB167	2.12	hypothetical protein	0.0187	-
TTHB170	0.40	hypothetical protein	0.0032	S
TTHB178	0.47	hypothetical protein	0.0051	L
TTHB185	0.23	hypothetical protein	0.0061	L
TTHB186	0.35	putative transcriptional regulator	0.0043	K
TTHB188	0.42	comserved hypothetical protein	0.0030	-
TTHB189	0.38	hypothetical protein	0.0095	-
TTHB191	0.41	hypothetical protein	0.0138	L
TTHB193	0.43	hypothetical protein	0.0038	L
TTHB195	0.49	hypothetical protein	0.0284	R
TTHB197	0.36	probable formate dehydrogenase	0.0057	C
TTHB201	2.01	transposase-like protein	0.0172	L
TTHB204	0.33	hypothetical protein	0.0242	K
TTHB209	0.48	ribonucleoside-diphosphate reductase, alpha subunit	0.0142	F
TTHB213	0.48	hypothetical protein	0.0340	-
TTHB230	0.45	putative ATP-dependent RNA helicase	0.0124	R
TTHB234	0.44	hypothetical protein	0.0103	-
TTHB237	0.35	2-hydroxymuconic semialdehyde hydrolase	0.0012	R
TTHB239	0.44	2-oxopent-4-dienoate hydratase	0.0094	Q
TTHB245	0.41	hypothetical protein	0.0089	I
TTHB246	0.42	4-hydroxy-2-ketovalerate aldolase	0.0010	E
TTHB249	0.44	phenol hydroxylase component A	0.0089	Q
TTHC001	9.22	putative RepA protein	0.0037	-
TTHC004	2.74	hypothetical protein	0.0041	-
TTHY060	4.26	conserved hypothetical protein	0.0205	-

In addition, the genes, whose expressions were affected by temperature downshift, were categorized according to functional categories used in COG database (http://www.ncbi.nlm.nih.gov/COG/old/palox.cgi?fun=all). Each gene function was categorized by using alphabets in COG database. Numbers of ≥2-fold up- and down-regulated genes ($q \leq 0.05$) in *T. thermophilus* HB8 at 30 s or 10 min after cold shock were classified in each category of COGs (Table 7). Total number of expression-changed genes increased about 5-fold at 10 min compared with at 30 s after cold shock. The number of down-regulated genes was larger than that of up-regulated ones both at 30 s and at 10 min after cold shock. Particularly, down-regulated genes involved in energy production and conversion (C in Table 7) were much increased at 10 min (46 genes) compared with 30 s (4 genes). Genes categorized into amino acid transport and metabolism (E) and coenzyme transport and metabolism (H) were also increased at 10 min. Suppression of energy production may affect other cellular activities such as amino acid transport and coenzyme transport.

Also, the percentage of these categorized genes is summarized in Fig. 5. The expression change was more remarkable at 10 min than 30 s for genes involved in translation (J), posttranscriptional modification, protein turnover, chaperones (O) and lipid transport and metabolism (I). Genes in these categories are related to reconstitute membrane fluidity, secondary structure of nucleic acids, protein folding and ribosome function damaged by temperature downshift. Thus, the cell may express these gene groups to overcome harmful effects caused by temperature downshift.

2. Expression of ttCSP1 and ttCSP2

Next, I focused on two CSPs of *T. thermophilus* HB8. As described above,

Table 7. Number of genes up- and down-regulated in *T. thermophilus* HB8 at 30 s or 10 min after cold shock in each category of COGs. Number of ORFs with a q value ≤ 0.05 and a fold change of ≥2-fold relative to those before cold shock have been listed.

Code	Description	30 s		10 min	
		Up (%)	Down (%)	Up (%)	Down (%)
J	Translation	1 (0.99)	3 (2.97)	12 (2.38)	36 (7.14)
K	Transcription	1 (0.99)	5 (4.95)	10 (1.98)	12 (2.38)
L	Replication, recombination and repair	2 (1.89)	1 (0.99)	13 (2.58)	9 (1.79)
B	Chromatin structure and dynamics	0 (0)	0 (0)	1 (0.20)	0 (0)
D	Cell cycle control, mitosis and meiosis	0 (0)	0 (0)	1 (0.20)	1 (0.20)
V	Defense mechanisms	1 (0.99)	1 (0.99)	3 (0.60)	5 (0.99)
T	Signal transduction mechanisms	0 (0)	3 (2.97)	10 (1.98)	1 (0.20)
M	Cell wall / membrane biogenesis	0 (0)	3 (2.97)	6 (1.19)	7 (1.39)
N	Cell motility	0 (0)	2 (1.98)	3 (0.60)	0 (0)
U	Intracellular trafficking and secretion	1 (0.99)	3 (2.97)	3 (0.60)	3 (0.60)
O	Posttranscriptional modification, protein turnover, chaperones	1 (0.99)	1 (0.99)	14 (2.78)	9 (1.79)
C	Energy production and conversion	5 (4.95)	4 (3.96)	6 (1.19)	46 (9.13)
G	Carbohydrate transport and metabolism	4 (3.96)	4 (3.96)	10 (1.98)	13 (2.58)
E	Amino acid transport and metabolism	2 (1.98)	8 (7.92)	8 (1.59)	28 (5.56)
F	Nucleotide transport and metabolism	0 (0)	0 (0)	3 (0.60)	5 (0.99)
H	Coenzyme transport and metabolism	1 (0.99)	1 (0.99)	3 (0.60)	15 (2.97)
I	Lipid transport and metabolism	1 (0.99)	0 (0)	5 (0.99)	11 (2.18)
P	Inorganic ion transport and metabolism	3 (2.97)	10 (9.9)	7 (1.39)	21 (4.17)
Q	Secondary metabolites biosynthesis, transport and catabolism	1 (0.99)	1 (0.99)	3 (0.60)	6 (1.19)
R	General function prediction only	6 (5.94)	5 (4.95)	27 (5.36)	29 (5.75)
S	Function unknown	4 (3.96)	1 (0.99)	13 (2.58)	13 (2.58)
-	Not in COGs	3 (2.97)	7 (6.93)	38 (7.54)	35 (6.94)
	Total (Up or Down)	37	64	199	305
	Total	101		504	

Up and Down indicate up- and down-regulated genes, respectively. The percentage of the altered genes in each category against total number is shown in parentheses.

transcription of the *ttcsp2* gene dramatically increased immediately after the temperature downshift. In contrast, transcription of *ttha0175* (*ttcsp1*) was not induced by temperature downshift (Fig. 6B). In the control experiment, expression level of *ttcsp1* and *ttcsp2* genes

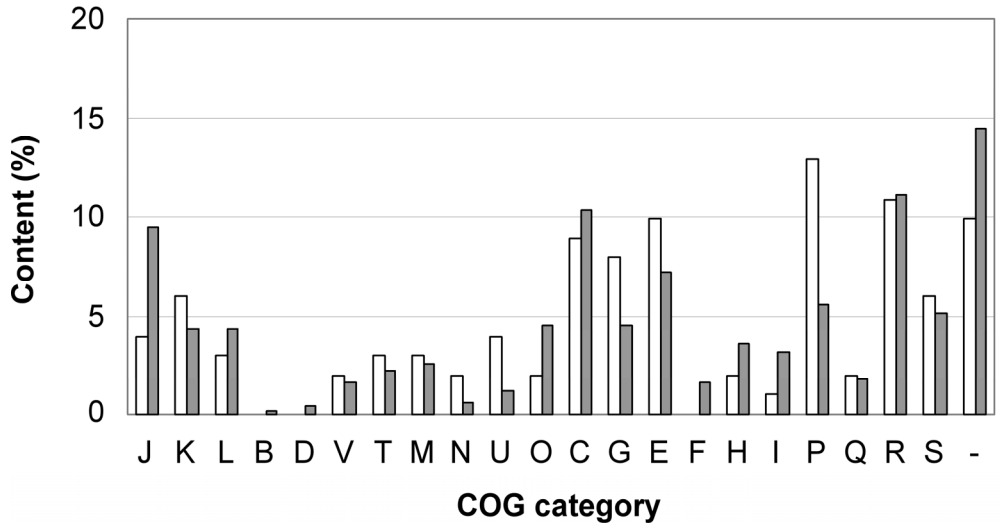

Fig. 5. COG category of genes up- and down-regulated at 30 s or 10 min after cold shock. The percentage of each COG-based categorized gene against total number of ≥2 fold expression-altered genes ($q \leq 0.05$) at 30 s (white bar) or 10 min (gray bar) after cold shock was shown. The definition for each COG code is given in Table 7.

remained constant from 0 to 10 min at 70°C (Fig. 6A). The mRNA expression level of *ttcsp2* was very low at 70°C, but increased to a similar level to that of *ttcsp1* after cold shock (Fig. 6C and D). Therefore, it was concluded that ttCSP1 and ttCSP2 were the cold-uninducible and cold-inducible CSP of *T. thermophilus* HB8, respectively. Similar high levels of expression to that of ttCSP2 have been observed for other cold-inducible CSPs (Etchegaray et al., 1996).

The difference in the expression between ttCSP1 and ttCSP2 was also found at protein expression level (Fig. 7, Table 8). The bands containing ttCSP1 were visible before and after the temperature downshift. In contrast, the band of ttCSP2 was at a detectable level at 30 min after cold shock. After 30 min, the expression levels of these two proteins were similar, which supported the DNA microarray results. Importantly, examination of the time course of expression showed time lag between mRNA and protein expression: the induction of *ttcsp2*

mRNA occurred at 30 s, whereas that of ttCSP2 proteins at 30 min. Time lag between mRNA and protein expression has been reported for other CSPs, although the time scales were different (Uppal et al., 2008). Such a time lag suggests that expression of ttCSP2 was controlled at the translational level. Melting of the secondary structure of *ttcsp2* mRNA by RNA helicase may be required for translation initiation.

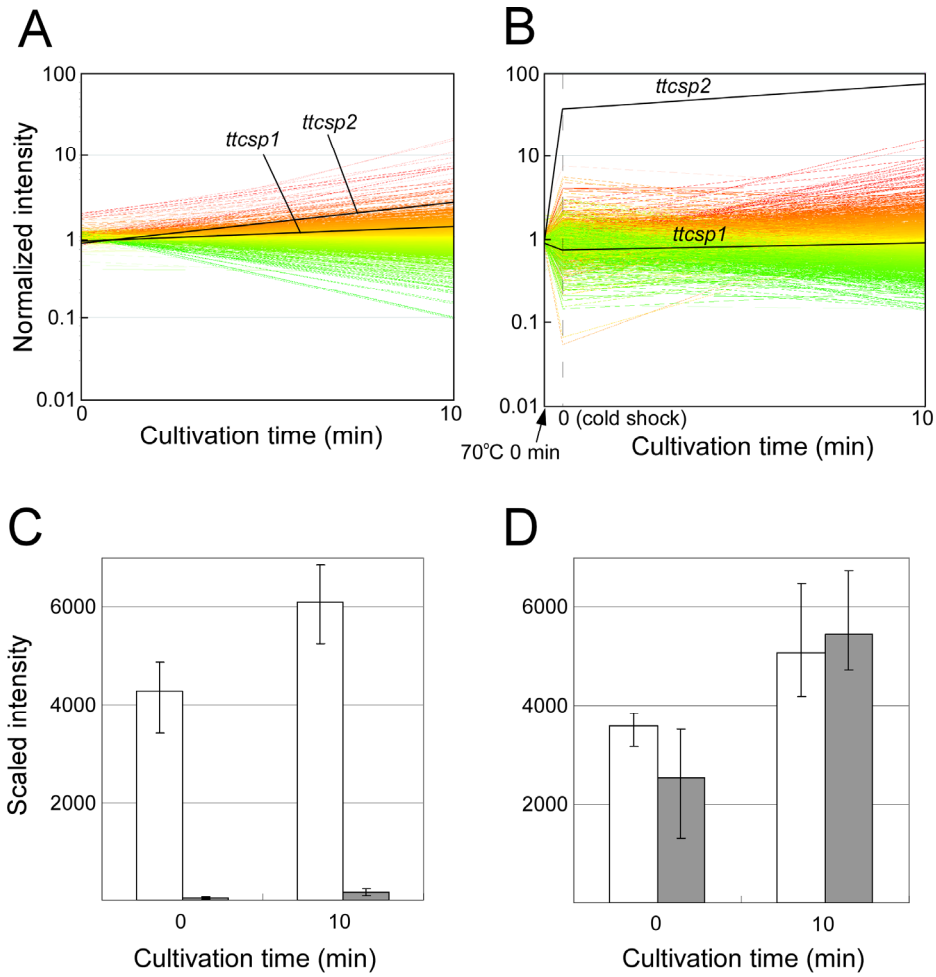

Fig. 6. Expression pattern of *ttcsp1* and *ttcsp2* genes. Expression patterns of all genes were displayed at 70°C (A) and 45°C (B). Green, yellow and red lines represent decreased expression, no change in expression and an increase in expression between 0 min (or before cold shock) and 10 min, respectively. The expression patterns of *ttcsp1* and *ttcsp2* genes are indicated by black lines. (C and D) Scaled intensities of *ttcsp1* and *ttcsp2* at 70°C and 45°C. In these panels, white and gray bars indicate intensities *ttcsp1* and *ttcsp2*, respectively. Scaled intensities of *ttcsp1* and *ttcsp2* genes were compared under each condition. Error bar means standard deviation for three independent analyses.

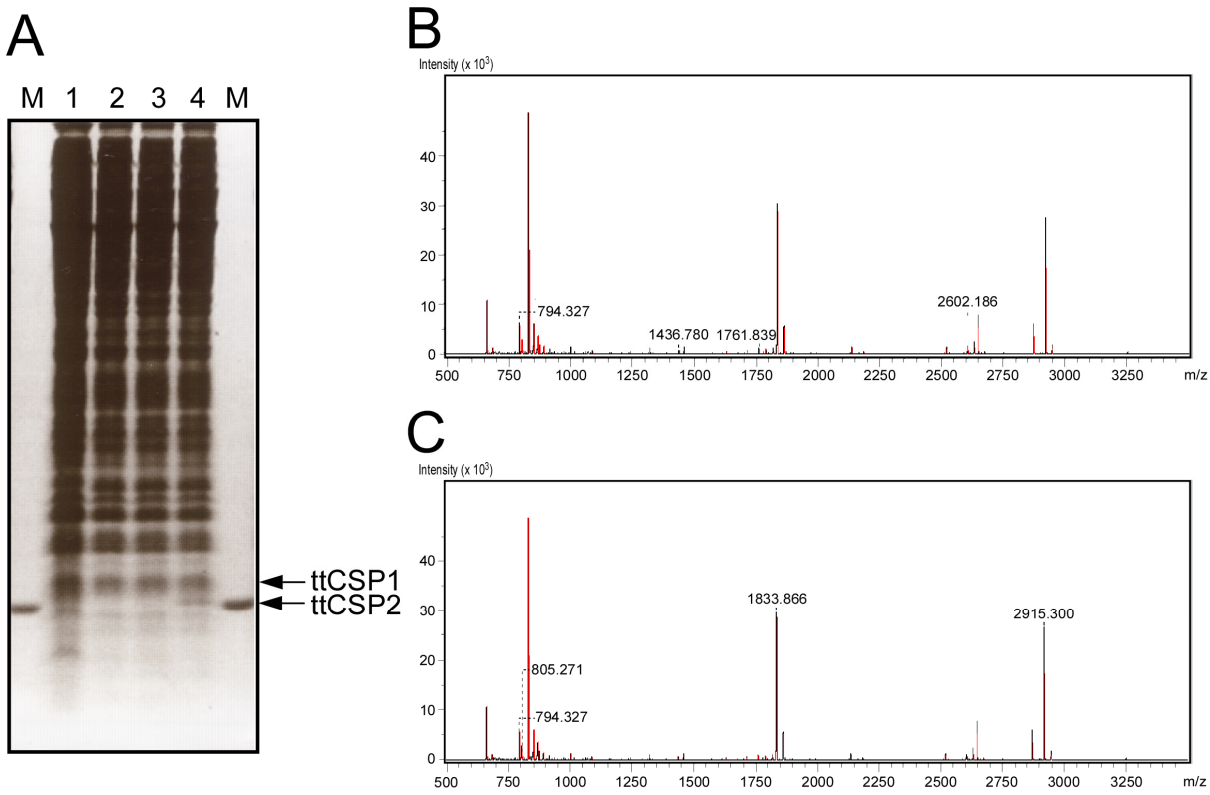

Fig. 7. Expression of ttCSP1 and ttCSP2 protein. (A) Tris-Tricine SDS-PAGE with lysates from *T. thermophilus* HB8. Each lane represents as follows: M, purified ttCSP2; 1, the lysate recovered from cells at 70°C for 0 min; 2, at 45°C for 0 min; 3, at 45°C for 10 min; and 4, at 45°C for 30 min. ttCSP1 (B) and ttCSP2 (C) were identified by MALDI-TOF MS. Black arrowed bands in the panel A were picked out and these peptide samples were prepared by in-gel digestion.

Table 8. Identification of ttCSP1 and ttCSP2 by MALDI-TOF MS.

Time point	Mowse score	Intensity coverage (%)	Sequence coverage (%)
ttCSP1			
45˚C 0 min	64	5.2	74.0
10 min	72	9.9	82.2
30 min	87	7.4	82.2
ttCSP2			
45˚C 30 min	56	34.3	70.6

3. Transcription start site of *ttcsp2* mRNA

The transcription start site of *ttcsp2* mRNA was determined to be 49 nt upstream from start codon by primer extension assay (Fig. 8). Namely, it was revealed that 5'-untranslated region (5'-UTR) of *ttcsp2* mRNA was 49 nt. The 5'-UTR of *ttcsp2* mRNA was much shorter than that of cold-inducible ecCspA, which was previously reported to be 166 or 165 nt (Tanabe et al., 1992). The 5'-UTR of *ttcsp2* mRNA showed no significant similarity to a "cold-box" sequence for other CSPs.

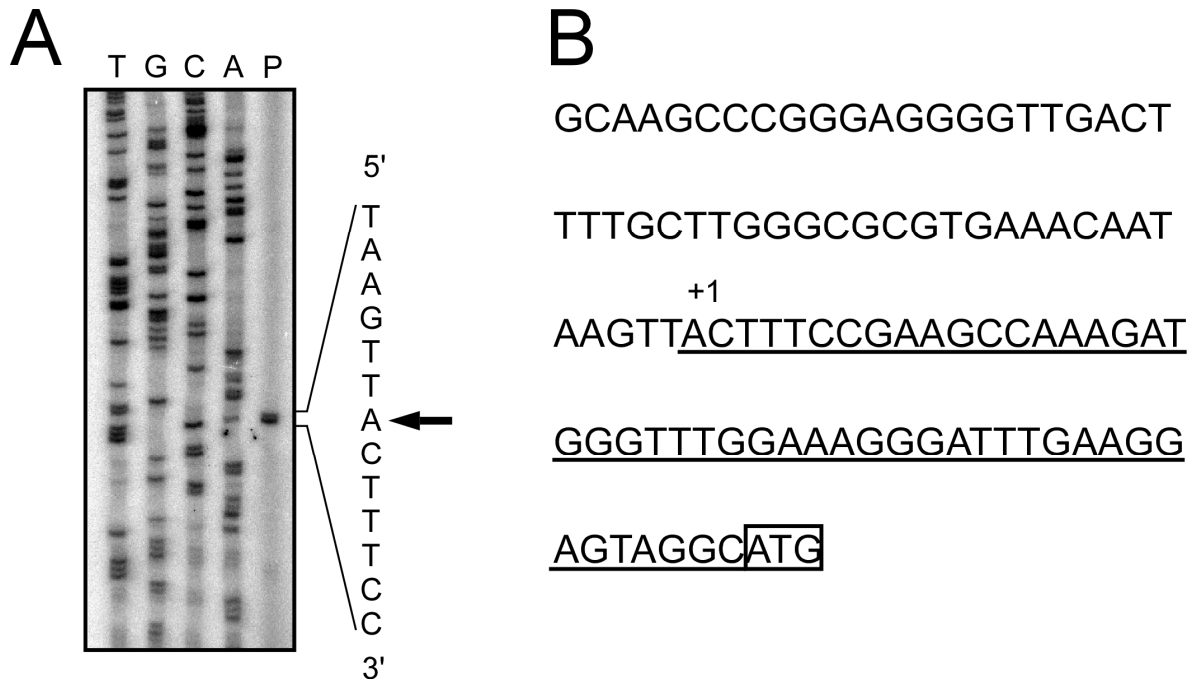

Fig. 8. Determination of the transcription start site of *ttcsp2*. (A) Primer extension assay was performed with total RNA at 45˚C at 10 min after cold shock. The primer extension product is indicated in lane P. The arrow indicates the start site. Lanes T, G, C and A represent *ttcsp2* sequencing reaction product, respectively. The primer extension and sequencing reaction products were subjected to 6% polyacrylamide-8 M urea gel. The sequence at the corresponding location in the gel is shown on the right. The detailed method is described in Materials and Methods. (B) The region upstream from start codon (squared sequence) of *ttcsp2* was shown. The underlined sequence and +1 represent the 5'-UTR of *ttcsp2* and the transcription start site, respectively.

4. Secondary structure in 5'-UTR of *ttcsp2* mRNA

Then, the secondary structure in the determined 5'-UTR of *ttcsp2* mRNA was predicted at 45˚C or 70˚C by using vsfold5 (Dawson et al., 2006). Interestingly, the 5'-UTR of *ttcsp2* mRNA was predicted to form two stable stem-loop structures at 45˚C (Fig. 9). The second stem-loop region was specific only at 45˚C and the structure was not formed at 70˚C. The secondary structure in 5'-UTR of *ttcsp2* mRNA may also function as a thermosensor, which senses intracellular temperature change. This RNA function was referred to as "RNA thermometer" and reported in some genes (Narberhaus et al., 2006). For example, in *E. coli rpoH*, mRNA conformation was changed by heat shock and translation was stimulated (Morita et al., 1999a; Morita et al., 1999b; Narberhaus et al., 2006). In addition, the secondary hairpin structure sequestered the SD-like sequence, which is a ribosomal RNA binding site in translation initiation (Fig. 9). Thus, to start translation, this hairpin structure should be melted. The time lag between *ttcsp2* mRNA increase and ttCSP2 expression

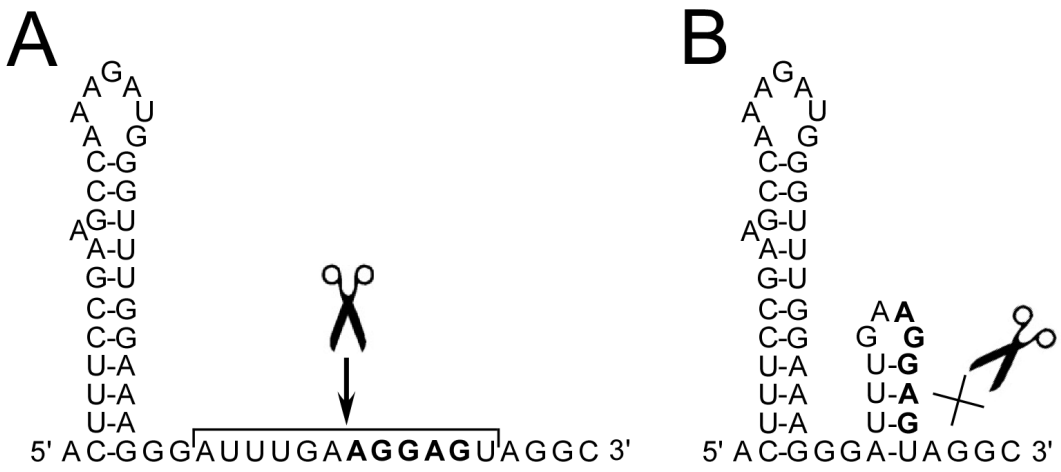

Fig. 9. The predicted secondary structures in 5'-UTR of *ttcsp2* mRNA. Panel A and B represent the predicted secondary structures at 70°C and 45°C, respectively. These structures were predicted by using vsfold5 (Dawson et al., 2006). A putative cleavage site targeted by endoribonuclease was indicated by a black arrow. The SD-like sequence was shown as bold letters.

(Fig. 6 and 7) is probably caused by the time to melt the hairpin structure. This suggested that translation of *ttcsp2* was controlled by the hairpin structure. Though ecCspA was difficult to be translated because SD sequence and start codon was sequestered in the stem-loop at 37˚C, the translation was stimulated when these sequence was released by temperature downshift (Giuliodori et al., 2010). This knowledge supports that translation of cold-incucible CSP can be regulated by the temperature-dependent secondary structure formation.

In contrast, no temperature-dependent stable stem-loop region was detected in the 5'-UTR of cold-uninducible *ttcsp1* mRNA (data not shown). This result led to the hypothesis that the secondary structure in the 5'-UTR of the *ttcsp2* mRNA represses its expression at 70°C, but can induce expression upon cold shock. One possibility is that secondary structure prevents an endoribonuclease to cleave the 5'-UTR.

5. Stabilization of *ttcsp2* mRNA in ttRNase deletion mutant

T. thermophilus HB8 has some ribonucleases (RNases) including RNase R and RNase II, but does not RNase E, an essential endoribonuclease in *E. coli*. In *T. thermophilus*, TTHA0252 was recently found as a novel RNase with both 5'-3' exoribonuclease and endoribonuclease activity (Ishikawa et al., 2006). Then, DNA microarray data of Δ*ttha0252* in early, middle and late log phases was analyzed. Scaled intensities of *ttcsp1* and *ttcsp2* mRNA were compared Δ*ttha0252* with wild-type strains (Fig. 10). Though the scaled intensity of *ttcsp1* mRNA in Δ*ttha0252* was similar to that in wild-type, that of *ttcsp2* mRNA was much higher in Δ*ttha0252* than wild-type at all growth phage examined. These results suggested that deletion of *ttha0252* prevented *ttcsp2* mRNA to be degraded and mRNA stabilized. Namely, TTHA0252 might regulate cellular level of *ttcsp2* mRNA at 70˚C by

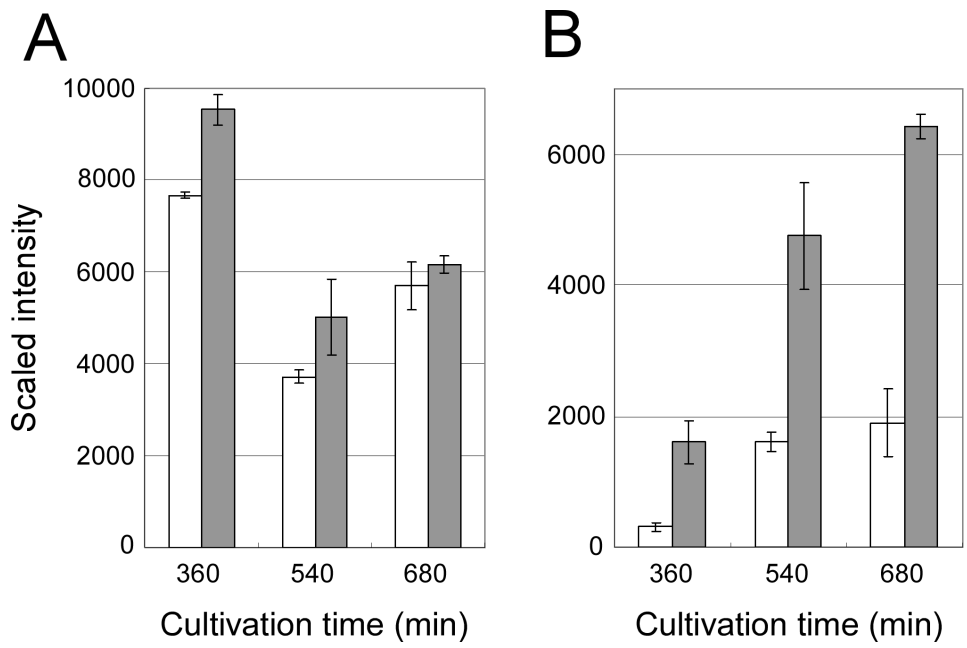

Fig. 10. Scaled intensities of *ttcsp1* (A) and *ttcsp2* (B) mRNA in wild-type and Δ*ttha0252*. In these panels, white and gray bars indicate intensities in wild-type and Δ*ttha0252*, respectively. Each time point represents early (360 min), middle (540 min) and late log phase (680 min), respectively. Scaled intensities of *ttcsp1* and *ttcsp2* genes were compared under each condition. Error bar means standard deviation.

recognizing the arrowed sequence (Fig. 9). Because the target sequence was occluded by the second hairpin structure, mRNA might avoid the degradation by TTHA0252 and accumulate at 45˚C. Similarly, the half-life of *eccspA* and *eccspE* mRNA became longer in *E. coli* strain with temperature-sensitive allele of RNase E than wild-type (Hankins et al., 2007; Uppal et al., 2008). Thus, endonuclease such as TTHA0252 was suggested to be important for regulation of *ttcsps* mRNA abundance.

6. Disruption of *ttcsp1* and *ttcsp2* genes

To investigate functional differentiation between ttCSP1 and ttCSP2, I constructed each single gene disruptant (Δ*ttcsp1* and Δ*ttcsp2*) and a double disruptant (Δ*ttcsp1/2*) of *T.*

thermophilus HB8. Deletion of *ttcsp1* and *ttcsp2* genes was confirmed by both genomic PCR and Southern blotting (Fig. 11). No band was observed in wild-type, but single specific band for *htk* or *hyg* was observed in all experiments. This suggested that target genes were disrupted at the exact position.

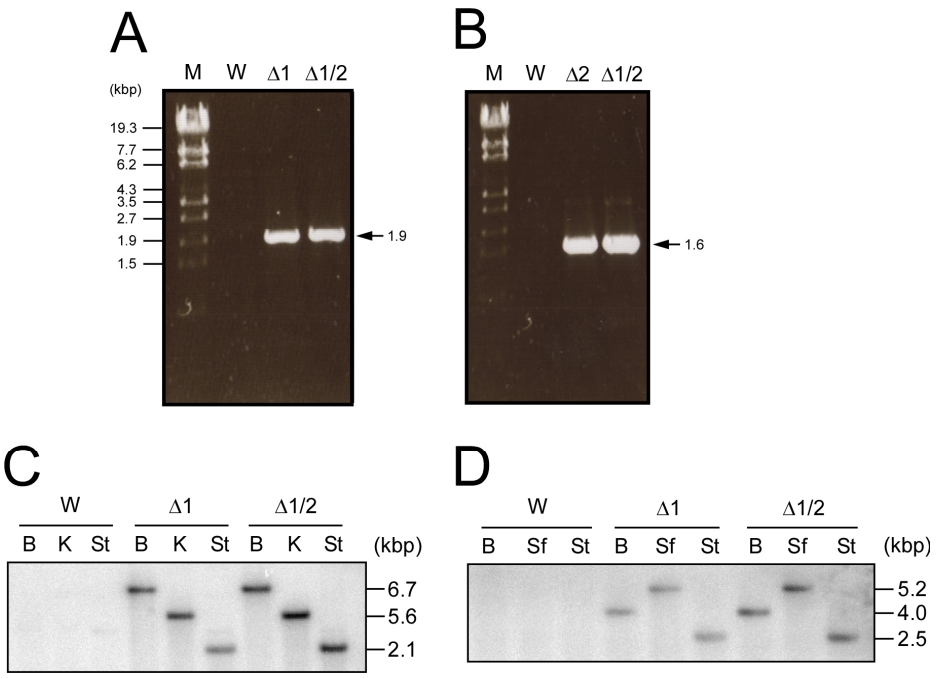

Fig. 11. Verification of *ttcsp1* and *ttcsp2* genes deletion. (A and B) Genomic PCR to confirm *ttcsp1* and *ttcsp2* gene deletion. The isolated chromosomal DNA from the wild-type (W), the Δ*ttcsp1* (Δ1), the Δ*ttcsp2* (Δ2) and Δ*ttcsp1/2* (Δ1/2) cells was used as template. The sizes (kbp) of λ/*Eco*T14I marker and mutant-specific bands are indicated in the left and right side of the gel, respectively. (C and D) Southern blotting to confirm *ttcsp1* and *ttcsp2* gene deletion. The isolated chromosomal DNA was digested with *Bam*H I (B), *Kpn* I (K), *Stu* I (St) and *Sfi* I (Sf). Then, the digested fragments were subjected to Southern blot analysis using *htk* or *hyg* as a probe. The fragmented chromosomal DNA from mutant cells showed the bands from *htk* or *hyg* though that from wild-type cells was absent.

To investigate the effect of *ttcsp1* and *ttcsp2* genes deletion for growth, wild-type and these deletion mutants strain were cultivated at 70°C and 45°C after cold shock (Fig. 12).

Growth of all strains was similar at 70°C. However, although growth of the single disruptants was almost identical to that of the wild-type strain until 300 min at 45°C after cold shock, growth of the disruptant after 300 min was slower than wild-type strain (Fig. 12C). This difference became evident after 1,020 min. These single deletion strains grew at 70°C and 45°C, indicating that ttCSP1 and ttCSP2 were not essential for growth even under cold conditions. However, growth of Δ*ttcsp1/2* was significantly delayed compared with the other strains. These results suggested that ttCSP1 might compensate for the lack of ttCSP2

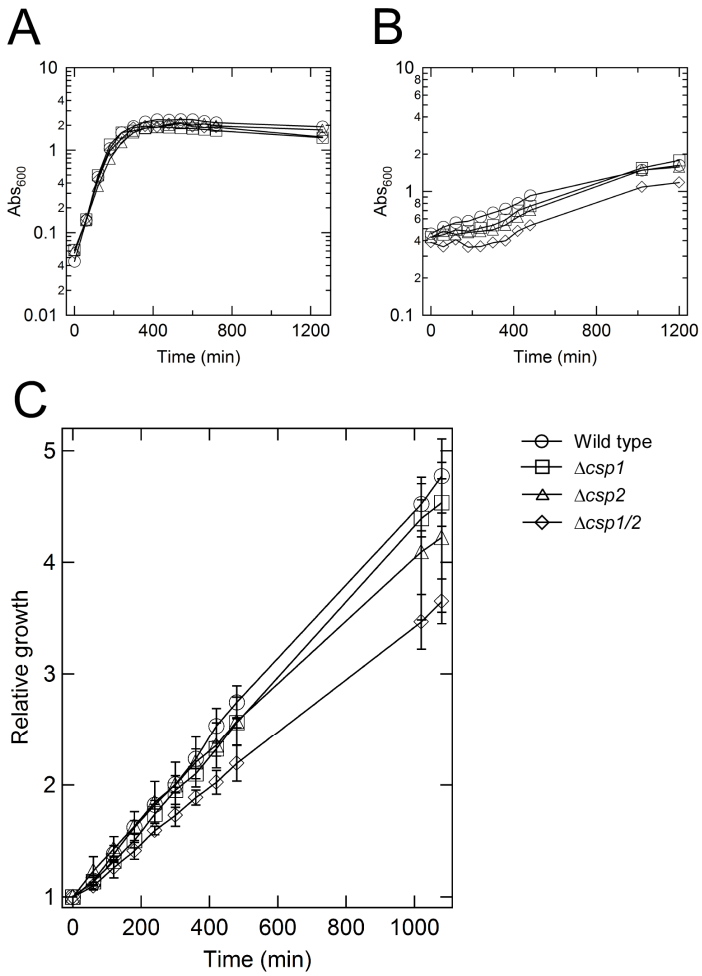

Fig. 12. Growth curve of wild-type and deletion mutants at 70°C (A) and 45°C (B) after cold shock. Markers represent as follows: circles, wild-type; squares, Δ*ttcsp1*; triangles, Δ*ttcsp2*; and diamonds, Δ*ttcsp1/2*. (C) Relative growth was shown as 1 at 0 min. Triplicate experiments were performed. Markers and error bars mean average values and standard deviation, respectively.

and *vice versa* under cold condition, although the mechanism of their cold-inducibility was different. It has been reported that cold-uninducible ecCspE compensated for the triple deletions of cold-inducible ecCspA, ecCspB and ecCspG (Xia et al., 2001). Thus, even though one CSP is down, other CSPs may be able to compensate for the functional failure because these have similar function each other.

7. DNA microarray analysis of Δ*ttcsp2* strain

To investigate transcriptional effects caused by *ttcsp2* deletion, DNA microarray analysis was performed in Δ*ttcsp2* compared with wild-type strain at 0.5, 10, 30 and 60 min after temperature downshift. Under these conditions, up- and down-regulated genes are shown in Tables 9-12. Also, the number of genes classified with COG category under each condition is listed in Table 13. The genes involved in translation (J), signal transduction mechanism, posttranscriptional modification, protein turnover (O), amino acid transport and metabolism (E) and inorganic ion transport and metabolism (P) were changed at 0.5 and 10 min (Table 9, 10 and 13). However, these genes observed are not regulated by ttCSP2 protein because expression of ttCSP2 protein was undetectable (Fig. 7). Thus, these genes are not probably regulated by ttCSP2 but other factors. ttCSP2 protein expresses and functions in the cell at 30 and 60 min according to Fig. 7. The genes involved in cell wall / membrane biogenesis (M, *ttha0641-0648*), survival proteins (*ttha0360-0363*) and amino acid transporter (*ttha0447-0452*) were regulated at 30 and 60 min (Table 11-13). This result was different from that of Δ*ttcsp1* (data not shown). This suggested that posttranscriptional regulation by ttCSP2 might relate to overcome membrane fluidity decrease caused by temperature downshift. Also, it was known that deletion mutant strain of survival proteins became sensitive against heat shock, high-osmotic and nutrient starvation stress (Li et al., 1994).

Survival proteins may be necessary for growth under various stress condition concluding low temperature. Furthermore, most of these genes were up-regulated in Δ*ttcsp2* strain (Table 13). This suggested that ttCSP2 could suppress transcripts of these gene groups in wild-type cell. Thus, ttCSP2 protein can negatively regulate these mRNAs as RNA chaperone at 30 and 60 min. To reveal this possibility, I must determine the 5'-UTR of these transcripts and investigate whether ttCSP2 binds to the sequences.

Table 9. Subset of genes up- and down-regulated in Δ*ttcsp2* strain at 30 s after cold shock. ORFs with a P-value ≤ 0.05 and a fold change of ≥1.5-fold relative to those in wild-type at the same time have been listed.

Locus tag	Fold	Annotation	P-value	COG code
TTHA0013	1.539	geranylgeranyl diphosphate synthetase	0.0485	H
TTHA0044	1.564	putative Na(+)/H(+) antiporter	0.00353	P
TTHA0111	1.927	hypothetical protein	0.0313	G E P R
TTHA0133	1.621	oxidoreductase, short-chain dehydrogenase/reductase family	0.0191	I Q R
TTHA0181	1.558	hypothetical protein	0.00188	-
TTHA0259	1.778	phosphate ABC transporter, periplasmid phosphate-biniding protein	0.0276	P
TTHA0260	2.83	probable phosphate ABC transporter, permease protein	0.00627	P
TTHA0261	1.884	probable phosphate ABC transporter, permease protein	0.0005	P
TTHA0262	1.865	probable phosphate ABC transporter, ATP-binding protein	0.0002	P
TTHA0270	0.467	carboxypeptidase	0.0197	E
TTHA0364	0.378	type IV pilus assembly protein PilF	0.00651	N U
TTHA0365	0.394	type IV pilus assembly protein, pilus retraction protein PilT	0.00966	N U
TTHA0366	0.535	aspartyl/glutamyl-tRNA(Asn/Gln) amidotransferase subunit B	0.0327	J
TTHA0397	1.58	hypothetical protein	0.0401	R
TTHA0455	0.626	rrf2 family protein, transcriptional regulator	0.0231	K
TTHA0456	0.614	cysteine desulfurase/cysteine sulfinate desulfinase	0.0068	E
TTHA0485	0.502	phosphoesterase-related protein	0.00434	T
TTHA0517	1.571	DedA family protein	0.0444	S
TTHA0518	1.666	TerC family protein	0.0442	P
TTHA0544	1.51	hypothetical protein	0.00615	L K J
TTHA0663	0.321	pyruvate orthophosphate dikinase	0.0448	G
TTHA0759	1.56	homoserine O-acetyltransferase	0.0446	E
TTHA0771	0.278	hypothetical protein	0.0296	E O T
TTHA0798	0.498	GGDEF domain protein	0.0489	T
TTHA0805	1.73	hypothetical protein	0.0425	-
TTHA0979	0.509	hypothetical protein	0.0467	G
TTHA0994	0.234	hypothetical protein	0.0208	-
TTHA0995	0.17	response regulator	0.00162	K T
TTHA1218	1.74	probable prepilin-like protein	0.0142	N T
TTHA1329	1.645	glutamine synthetase	0.0376	E
TTHA1334	1.627	branched-chain amino acid ABC transporter, ATP-binding protein	0.0175	E

TTHA1408	0.637	ABC transporter, ATP-binding protein	0.0236	V	
TTHA1422	3.029	thioredoxin	0.00785	O	C
TTHA1447	0.619	alanine dehydrogenase	0.0295	E	
TTHA1452	1.509	non-discriminating and archaeal-type aspartyl-tRNA synthetase	0.0235	J	
TTHA1498	0.617	elongation factor G (EF-G-2)	0.0181	J	
TTHA1533	1.568	hypothetical protein	0.00311	-	
TTHA1570	1.646	deoxyhypusine synthase	0.0295	O	
TTHA1651	0.65	maltose ABC transporter, permease protein	0.00386	G	
TTHA1679	1.508	30S ribosomal protein S14	0.012	J	
TTHA1708	1.732	hypothetical protein	0.0394	I	
TTHA1742	1.593	orotate phosphoribosyltransferase	0.0291	F	
TTHA1838	0.207	SufC protein (ATP-binding protein)	0.0322	O	
TTHA1839	0.165	SufB protein (membrane protein)	0.0287	O	
TTHA1840	0.158	SufD protein (membrane protein)	0.0247	O	
TTHA1841	0.139	putative dioxygenase ferredoxin subunit	0.0222	P	R
TTHA1864	1.702	S-layer protein-related protein	0.0264	-	
TTHA1910	1.647	probable homoaconitase small subunit (homoaconitate hydratase)	0.02	E	
TTHB030	0.49	probable sugar transporter	0.0434	G	
TTHB067	2.888	alkaline phosphatase	0.0208	P	
TTHB070	3.447	survival protein SurE	0.00129	R	
TTHB071	4.649	hypothetical protein	0.00501	G	
TTHB094	0.544	putative short-chain oxidoreductase	0.0239	-	
TTHB177	0.582	iron ABC transporter, periplasmic iron-binding protein	0.0199	P	
TTHB179	0.398	hypothetical protein	0.037	S	
TTHB181	0.315	hypothetical protein	0.0212	-	
TTHB189	0.471	hypothetical protein	0.0228	-	
TTHB196	0.638	putative protein required for formate dehydrogenase activity	0.0359	C	
TTHB228	0.54	hypothetical protein	0.0366	-	
TTHB229	0.561	hypothetical protein	0.0448	-	
TTHB230	0.581	putative ATP-dependent RNA helicase	0.0445	R	
TTHB245	0.665	hypothetical protein	0.035	I	

Table 10. Subset of genes up- and down-regulated in Δ*ttcsp2* strain at 10 min after cold shock. ORFs with a P-value ≤ 0.05 and a fold change of ≥1.5-fold relative to those in wild-type at the same time have been listed.

Locus tag	Fold	Annotation	P-value	COG code	
TTHA0156	1.903	hypothetical protein	0.0113	K	
TTHA0202	1.535	hypothetical protein	0.0167	S	
TTHA0255	1.707	ferric uptake regulation protein	0.0125	P	
TTHA0287	1.518	2-oxoglutarate dehydrogenase E3 component (dihydrolipoamide dehydrogenase)	0.0379	C	
TTHA0360	0.566	survival protein SurE	0.00245	R	
TTHA0395	1.734	hypothetical protein	0.00475	-	
TTHA0620	1.511	alternative anthranilate synthase component I+II (TrpEG)	0.0227	E	H
TTHA0669	1.961	phosphoadenosine phosphosulfate reductase (CysH)	0.0235	E	H
TTHA0792	0.646	hypothetical protein	0.0424	K	
TTHA0970	0.648	phenylacetic acid degradation protein PaaC	0.0196	S	
TTHA1210	1.705	2-isopropylmalate synthase (LeuA)	0.0248	E	
TTHA1332	1.543	branched-chain amino acid ABC transporter, permease protein	0.0213	E	
TTHA1334	1.65	branched-chain amino acid ABC transporter, ATP-binding protein	0.0178	E	
TTHA1337	1.679	peptide ABC transporter, permease protein	0.0331	E	P
TTHA1417	2.134	sulfur oxidation protein SoxB	0.00997	F	
TTHA1418	6.018	putative cytochrome c	0.00074	C	
TTHA1419	4.956	putative cytochrome c precursor	0.00639	C	
TTHA1420	7.525	sulfur oxidation protein SoxZ	0.0143	-	
TTHA1421	6.394	sulfur oxidation protein SoxY	0.0159	S	
TTHA1422	9.453	thioredoxin	0.0128	O	C
TTHA1669	1.506	translation initiation factor 1 (IF-1)	0.0467	J	
TTHA1671	1.758	adenylate kinase	0.0243	F	
TTHA1672	1.516	preprotein translocase SecY subunit	0.0122	U	
TTHA1759	1.947	hypothetical protein	0.0347	S	
TTHA1839	0.229	SufB protein (membrane protein)	0.0465	O	
TTHA1840	0.209	SufD protein (membrane protein)	0.0318	O	
TTHA1841	0.182	putative dioxygenase ferredoxin subunit	0.0387	P	R
TTHA1903	1.646	putative acetylglutamate kinase	0.0209	E	
TTHA1904	1.599	N-acetyl-gamma-glutamyl-phosphate reductase	0.0489	E	
TTHA1944	1.874	hypothetical protein	0.0388	S	
TTHB021	1.7	hypothetical protein	0.0481	V	
TTHB028	0.633	hypothetical protein	0.0343	C	
TTHB030	0.556	probable sugar transporter	0.0117	G	
TTHB068	1.689	hypothetical protein	0.026	J	
TTHB094	0.625	putative short-chain oxidoreductase	0.0365	-	
TTHB101	0.61	phytoene synthase	0.0476	I	
TTHB120	1.682	hypothetical protein	0.0336	-	
TTHB182	0.369	hypothetical protein	0.0252	-	
TTHB183	0.329	hypothetical protein	0.0329	-	

Table 11. Subset of genes up- and down-regulated in Δ*ttcsp2* strain at 30 min after cold shock. ORFs with a P-value ≤ 0.05 and a fold change of ≥1.5-fold relative to those in wild-type at the same time have been listed.

Locus tag	Fold	Annotation	P-value	COG code		
TTHA0035	1.668	hypothetical membrane protein	0.00344	-		
TTHA0360	0.182	survival protein SurE	5.3E-05	R		
TTHA0361	0.253	survival protein SurE	2.1E-06	R		
TTHA0362	0.335	hypothetical protein	0.00001	S		
TTHA0363	0.509	putative hydrolase, HAD superfamily	3.4E-05	R		
TTHA0471	1.589	peptide ABC transporter, permease protein	0.00522	E	P	
TTHA0641	1.593	hypothetical protein	0.0061	M		
TTHA0645	1.602	putative glycosyltransferase	0.00033	M		
TTHA0646	2.264	hypothetical protein	0.00819	-		
TTHA0647	1.603	putative glycosyltransferase	0.00014	M		
TTHA0648	1.565	probable glycosyltransferase	0.00044	M		
TTHA0742	1.735	hypothetical protein	0.00114	-		
TTHA0743	1.637	glycosyltransferase related protein	0.0199	M	N	U
TTHA0773	1.543	hypothetical protein	0.00331	-		
TTHA0843	1.518	serine protein kinase	0.0289	T		
TTHA1268	0.643	hypothetical protein	3.8E-05	-		
TTHA1338	1.636	ABC transporter permease protein	0.00655	E	P	
TTHA1414	1.816	putative sulfurtransferase	0.00236	P		
TTHA1443	0.587	hypothetical protein	0.00906	S		
TTHA1584	1.579	Type II restriction enzyme TthHB8I (endonuclease TthHB8I) (R.TthHB8I)	0.00083	-		
TTHB074	1.737	putative C4-dicarboxylate transporter, periplasmic C4-dicarboxylate-binding protein	0.00634	G		
TTHB077	0.655	oxidoreductase, short-chain dehydrogenase/reductase family	0.0461	I	Q	R
TTHB080	1.948	2-deoxy-D-gluconate 3-dehydrogenase	0.0364	I	Q	R
TTHB175	2.077	ABC transporter, ATP-binding protein	0.00015	E		
TTHC001	1.736	putative RepA protein	0.0003	-		

Table 12. Subset of genes up- and down-regulated in Δ*ttcsp2* strain at 60 min after cold shock. ORFs with a P value ≤ 0.05 and a fold change of ≥1.5-fold relative to those in wild-type at the same time have been listed.

Locus tag	Fold	Annotation	P-value	COG code
TTHA0034	1.508	hypothetical protein	0.0137	-
TTHA0035	1.791	hypothetical membrane protein	0.00082	-
TTHA0036	1.608	hypothetical protein	9.4E-06	S
TTHA0206	0.645	nicotinamide nucleotide transhydrogenase, alpha subunit 1	0.047	C
TTHA0354	0.64	ABC transporter, permease protein, MalFG family	0.0349	G
TTHA0362	0.526	hypothetical protein	0.0257	S
TTHA0447	1.526	branched-chain amino acid transporter ATP-binding protein	0.00973	E
TTHA0449	1.718	branched-chain amino acid ABC transporter, permease protein	0.0121	E
TTHA0450	1.561	branched-chain amino acid ABC transporter, permease protein	0.0082	E
TTHA0452	1.643	branched-chain amino acid ABC transporter, ATP-binding protein	7.4E-05	E
TTHA0647	1.523	putative glycosyltransferase	0.00255	M
TTHA0690	1.521	acetyl-CoA acetyltransferase	0.0133	I
TTHA0797	0.602	(s)-2-hydroxy-acid oxidase subunit (GlcD)	0.035	C
TTHA0828	0.642	hypothetical protein	0.00148	-
TTHA0859	1.51	uridylate kinase	0.00874	F
TTHA0910	1.56	exoribonuclease	0.0007	K
TTHA0943	1.566	hypothetical protein	0.0137	-
TTHA0945	1.613	hypothetical protein	0.0136	-
TTHA0947	1.725	triosephosphate isomerase	0.00428	G
TTHA1102	0.616	hypothetical protein	0.0037	-
TTHA1117	1.52	iron-sulfur protein	0.00208	C
TTHA1222	0.54	pilin, type IV, putative	0.00025	-
TTHA1319	0.652	probable acetyltransferase	0.00853	R
TTHA1766	0.612	S-layer-like protein	0.0257	-
TTHA1918	1.632	hypothetical protein	0.0439	-
TTHA1920	1.616	thioredoxin reductase	0.00249	O
TTHB088	0.652	Zn-dependent hydrolase	0.0164	R
TTHB089	0.604	hypothetical protein	0.0498	-
TTHB227	1.555	hypothetical protein	0.0196	-

Table 13. Number of genes up- and down-regulated in *T. thermophilus* HB8 at 0.5, 10, 30 and 60 min after cold shock in each category of COGs. Number of ORFs with a P-value ≤ 0.05 and a fold change of ≥1.5-fold relative to those in wild-type at the same time have been listed.

Code	Description	30 s		10 min		30 min		60 min	
		Up	Down	Up	Down	Up	Down	Up	Down
J	Translation	3	2	2	0	0	0	0	0
K	Transcription	1	2	1	1	0	0	1	0
L	Replication, recombination and repair	1	0	0	0	0	0	0	0
V	Defense mechanisms	0	1	1	0	0	0	0	0
T	Signal transduction mechanisms	1	4	0	0	1	0	0	0
M	Cell wall / membrane biogenesis	0	0	0	0	5	0	1	0
N	Cell motility	1	2	0	0	1	0	0	0
U	Intracellular trafficking and secretion	0	2	1	0	1	0	0	0
O	Posttranscriptional modification, protein turnover, chaperones	2	4	1	2	0	0	1	0
C	Energy production and conversion	1	1	4	1	0	0	1	2
G	Carbohydrate transport and metabolism	2	4	0	1	1	0	1	1
E	Amino acid transport and metabolism	5	4	8	0	3	0	4	0
F	Nucleotide transport and metabolism	1	0	2	0	0	0	1	0
H	Coenzyme transport and metabolism	1	0	2	0	0	0	0	0
I	Lipid transport and metabolism	2	1	0	1	1	1	1	0
P	Inorganic ion transport and metabolism	8	2	2	1	3	0	0	0
Q	Secondary metabolites biosynthesis, transport and catabolism	1	0	0	0	1	1	0	0
R	General function prediction only	4	2	0	2	1	4	0	2
S	Function unknown	1	1	4	1	0	2	1	1
-	Not in COGs	4	6	3	3	6	1	6	5
	Total (Up or down)	39	38	31	13	24	9	18	11
	Total	77		44		33		29	

8. Thermal stability of ttCSP1 and ttCSP2

Thermal stability of ttCSP1 and ttCSP2 secondary structures was examined by monitoring the ellipticity at 216 nm from 25˚C to 95˚C (Fig. 13, solid lines). These results indicated that these proteins were stable to about 70˚C. Also, ttCSP1 and ttCSP2 refolded as temperature changed from 95˚C to 25˚C (Fig. 13, dashed lines). Consequently, it was revealed that both ttCSP1 and ttCSP2 underwent the reversible thermal-denaturation pattern. It was reported that thermal denaturation process of ecCspA was also reversible (Reid et al., 1998). This process may be characteristic to CSPs with low-molecular weight.

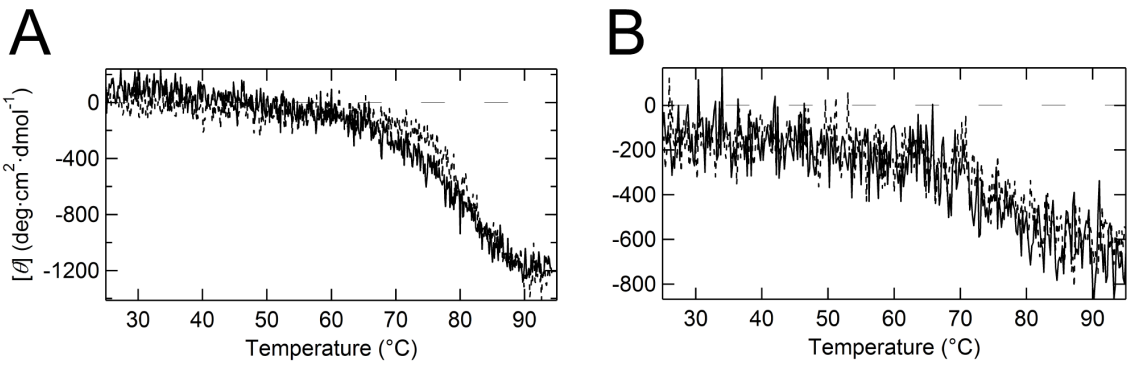

Fig. 13. CD spectral change of ttCSP1 (A) and ttCSP2 (B). CD values of ttCSP1 and ttCSP2 were measured at 216 nm from 25˚C to 95˚C (solid lines) and from 95˚C to 25˚C (dashed lines) to investigate thermal-reversibility. The detailed method is described in Materials and Methods.

9. Oligomeric structure of ttCSP1 and ttCSP2

In order to examine an interaction between ttCSPs and DNA, analytical size-exclusion chromatography was carried out using dT7 or dT31 (7 or 31-nt oligo-dT) (Fig. 14). In the absence of DNA, ttCSP1 and ttCSP2 were eluted at the volume corresponding to an apparent molecular weight of 7,300 and 8,200, judging from the calibration curve. As the calculated molecular weight of ttCSP1 and ttCSP2 are 8,200 and 7,800, respectively, ttCSP1 and ttCSP2

was considered to exist as a monomer in solution. In the presence of dT7 (apparent M.w. 10,100), the elution peaks of ttCSP1 and ttCSP2 were shifted to elution volumes corresponding to a molecular weight of around 15,700 (Table 14). This indicated that one molecule of ttCSP1 and ttCSP2 could form a complex with one molecule of dT7. Furthermore, the elution peaks of ttCSP1 and ttCSP2 were shifted to elution volumes corresponding to a molecular weight of around 47,900 and 45,500, respectively, in the presence of dT31 (apparent M.w. 30,600) (Table 14). This indicated that two molecules of ttCSP1 and ttCSP2 could form a complex with one molecule of dT31. It was reported that the DNA-binding site in CspB from *B. subtilis* or Csp from *B. caldolyticus* (bcCsp) interacts with 6-7 nucleotides (Max et al., 2006; Max et al., 2007). Thus, these results suggest that multiple molecules of ttCSP1 and ttCSP2 may bind to ssDNA longer than 7-nt.

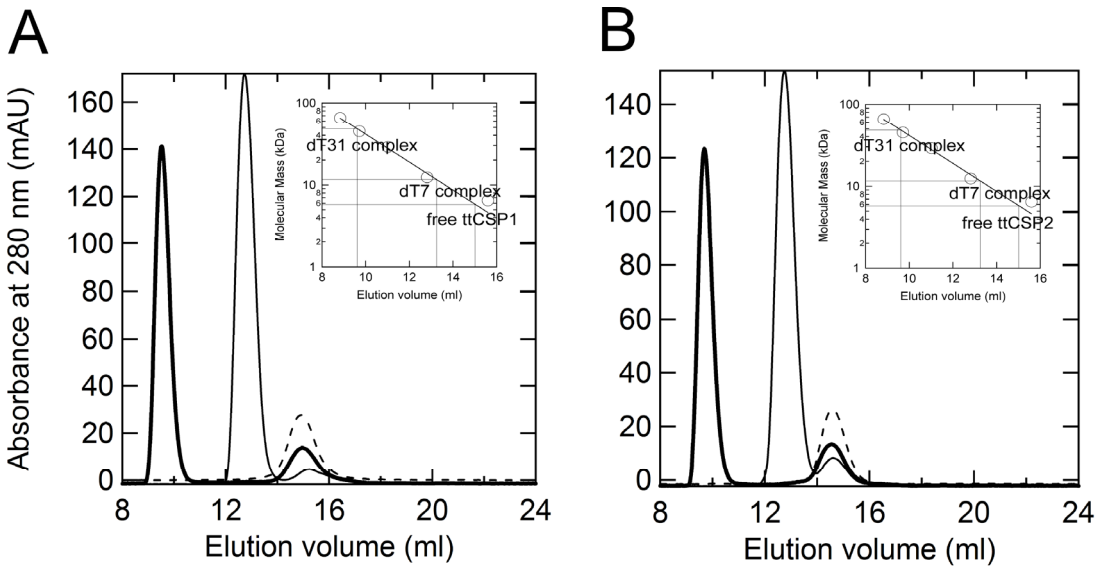

Fig. 14. Size-exclusion chromatography of ttCSP1 and ttCSP2. Panel A and B represent the elution profiles of ttCSP1 and ttCSP2, respectively. Bold, solid and dashed lines indicate the mixture with dT31, dT7 and free protein, respectively. The inset shows the calibration curve. Standard proteins were used: albumin from bovine serum, 66 kDa; albumin from chicken egg, 45 kDa; carbonic anhydrase from bovine erythrocytes, 29 kDa; cytochrome c from horse heart, 12.4 kDa; aprotinin from bovine lung, 6.5 kDa.

Table 14. Molar ratio of complex of ttCSP1 and ttCSP2 with dT7 or dT31 in solution.

Protein and ligands	Elution volume (ml)	Apparent M.w. (kDa)	Molar ratio
dT7	14.0	10.1	-
dT31	10.8	30.6	-
ttCSP1	14.9	7.3	-
ttCSP2	14.6	8.2	-
ttCSP1 + dT7	12.7	15.7	1:1
ttCSP2 + dT7	12.7	15.7	1:1
ttCSP1 + dT31	9.5	47.9	2:1
ttCSP2 + dT31	9.7	45.5	2:1

10. Nucleic acid-binding affinity

To further investigate the difference between ttCSP1 and ttCSP2, we examined nucleic acid-binding properties of these proteins. Nucleic acid-binding affinity was determined by using fluorescence quenching of a Trp residue. The K_d values calculated from fluorescence intensity in this experiment are shown in Table 15. The K_d of ttCSP1 and ttCSP2 were lower for thymine than the other four bases among 7-nt oligonucleotides. As for dT oligonucleotides, the K_d values decreased as the length of oligonucleotides increased. These results suggested that both ttCSP1 and ttCSP2 preferred thymine to the other bases and displayed the strong affinity for longer DNA molecules. These results are consistent with previous studies about CSPs from *E. coli* and *B. subtilis* (Johnston et al., 2006; Lopez et al., 1999). Moreover, in many cases the K_d of ttCSP1 for oligo(ribo)nucleotides was lower than that of ttCSP2. In particular, the affinity of ttCSP1 to stem-loop structures was significantly higher (2-fold~28-fold) than ttCSP2. The difference in the affinity to nucleic acids between ttCSP1 and ttCSP2 may be ascribable to difference in their oligonucleotide-binding sites. Sequence identity between these CSPs is 69%, suggesting significant structural differentiation.

Table 15. The K_d for various single-stranded DNA (ssDNA) and RNA.
The numbers in ssDNA (RNA) column represent the length of nucleic acids.

	K_d (nM)	
ssDNA (RNA)	ttCSP1	ttCSP2
dT3	14300 ± 1600	15600 ± 3000
dT4	2500 ± 190	7000 ± 820
dT5	340 ± 180	1590 ± 78
dT6	12 ± 0.9	56 ± 3
dT7	20 ± 1.2	54 ± 3
dT8	0.56 ± 0.01	21 ± 2
dT10	4.8 ± 0.3	2.0 ± 0.2
dA7	1260 ± 170	2640 ± 530
dA31	1200 ± 280	520 ± 90
dC7	8300 ± 440	22100 ± 1420
dC31	260 ± 9	1900 ± 60
dG7	3600 ± 860	3270 ± 450
dG31	3040 ± 680	18700 ± 470
U7	85 ± 7	770 ± 70
LoopdT7	31 ± 7	400 ± 22
LoopdT7dA4	32 ± 7	257 ± 12
LoopdT11	31 ± 7	854 ± 37
Stem5dT7	59 ± 11	104 ± 5
Stem3dT7	22 ± 7	84 ± 15

Then, I discussed the difference between ttCSP1 and ttCSP2 based on the ttCSP1 crystal structure (published elsewhere) and a homology model of ttCSP2 structure, which was constructed with Modeller. A model structure of ttCsp1-dT6 was constructed based on bcCsp-dT6 (PDB code 2HAX) (Max et al., 2007). Since two bcCsp molecules (A and B chains) form a domain-swap dimer, the main-chain atoms were superimposing LSQKAB in CCP4 (Kabsch et al., 1976) as follows: 2-21 of ttCSP1, 2-21 of bcCsp A chain; 25-37 of ttCsp1, 25-37 of bcCsp A chain; 38-55 of ttCSP1, 38-55 of bcCsp B chain; and 58-68 of ttCSP1, 56-66 of bcCsp B chain. According to these structures, a positively charged region

(Fig. 15, dashed circle) can be found on the surface of the protein near the putative oligonucleotide-binding site of ttCSP1, but not ttCSP2. This region was presumed to be located on the 5'-side stem region of stem3dT7. Thus, ttCSP1 can strongly recognize the stem region at 5'-side of continuous T sequences in a secondary structure-forming DNA compared with ttCSP2.

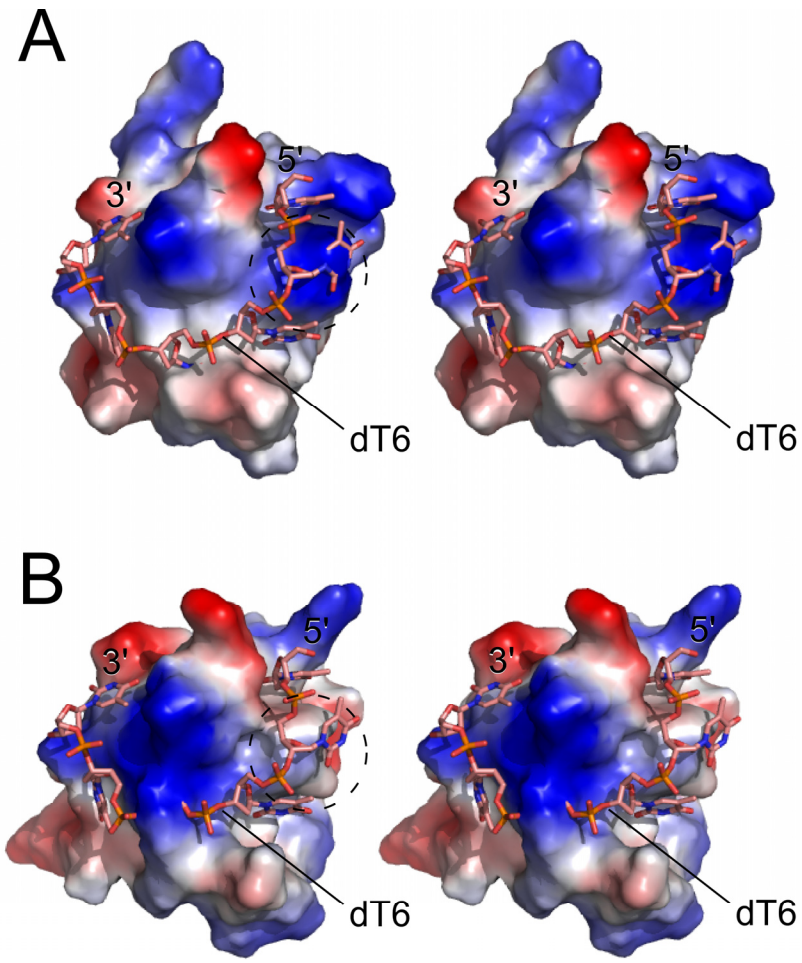

Fig. 15. The ttCSP1 crystal structure (A) and a homology model of ttCSP2 (B). The figures are drawn in stereo. Both molecules are shown along with the electron potential map on a scale from negative (red) to positive (blue). In (A) and (B), a short ssDNA (dT6) was modelled on the surface of ttCSP1 and ttCSP2 molecules based on the structure of bcCsp complex with dT6 (PDB code 2HAX).

11. DNA-melting activity

To investigate the ability of ttCSP1 and ttCSP2 to bind to dsDNA, EMSA was performed with the mixtures of ttCSP1 or ttCSP2 with 21f-21r dsDNA. ttCSP1(ttCSP2)-DNA complex was monitored by detecting the bands of these proteins bound to the radiorabeled dsDNA (Fig. 16). Consequently, the band of the ttCSP1-DNA complex was observed, but ttCSP2 was not. The band of ttCSP1-DNA complex was migrated at the similar position to that of ttCSP1-ssDNA complex. Since it was shown that ttCSP1 did not bind to 21f ssDNA but bound to 21r (data not shown), this result suggested that ttCSP1 did not directly bind to 21f-21r dsDNA but bound to 21r ssDNA after melting the double strand. This result is consistent with previous studies about ecCspE (Phadtare et al., 2002a; Phadtare and Severinov, 2005). It was reported that ecCspE melted double-stranded nucleotide and functioned as a transcription antiterminator (Bae et al., 2000; Phadtare et al., 2002a; Phadtare et al., 2002b). Thus, it is possible that ttCSP1 binds to the upstream region of an appropriate target gene and inhibits the formation of a hairpin structure by binding to thymine-rich stretches (Fig. 17).

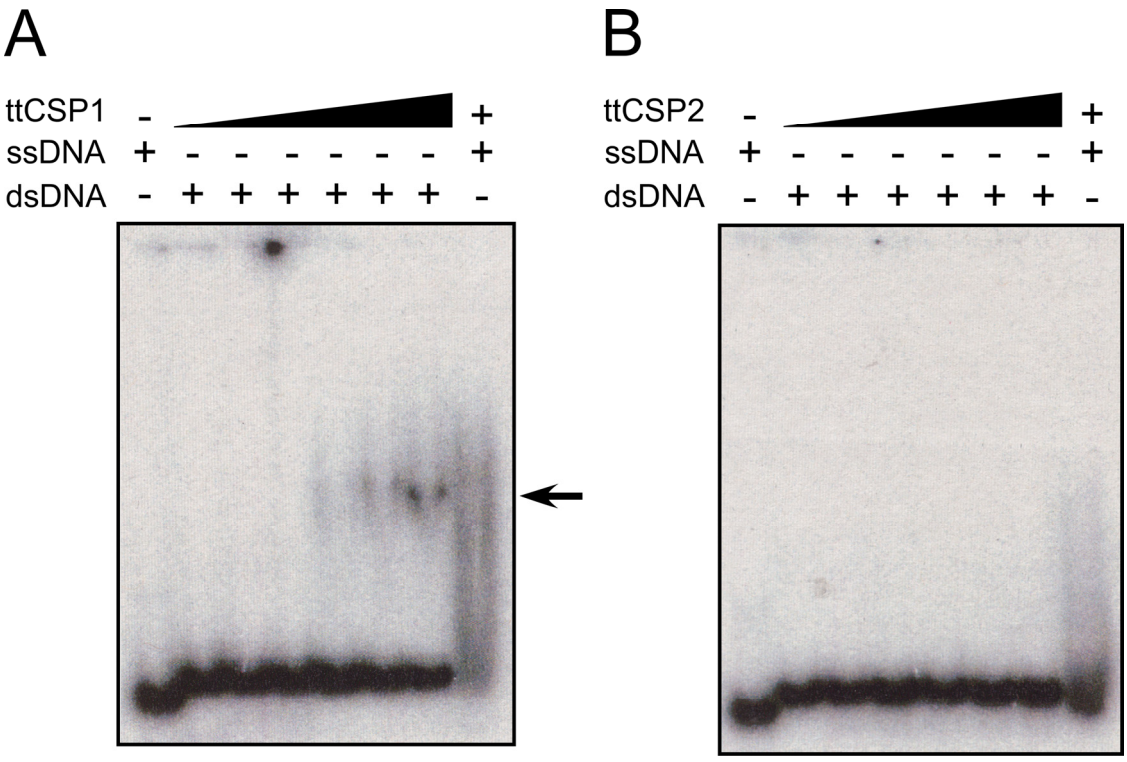

Fig. 16. EMSA of the mixtures of ttCSP1 (A) or ttCSP2 (B) with dsDNA. The mixtures of 10 μM ttCSP1 or ttCSP2 with 1 μM ssDNA (21r) were loaded in the right end lane of panel A and B. The substrate 21f-21r dsDNA was incubated with 0.5, 1.0, 10, 20, 50 μM of ttCSP1 or ttCSP2 at 25˚C for 5 min. The detailed method is described in Materials and Methods. The black arrow represents the ttCSP1-21r complex.

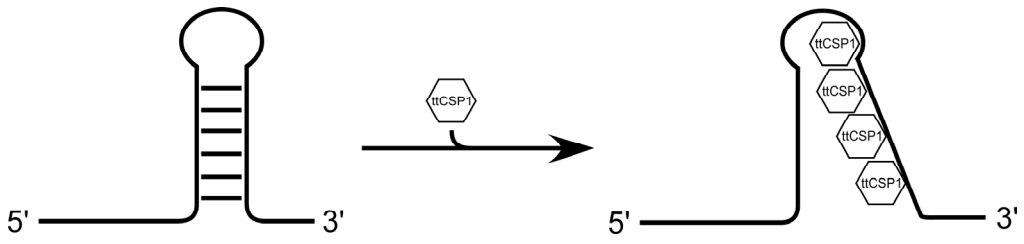

Fig. 17. Melting activity of ttCSP1 against secondary structured RNA.

Conclusion

Transcriptome analysis revealed that the mRNA expression level of *ttcsp2* was dramatically increased after temperature downshift compared with that of *ttcsp1* which was constitutively expressed. To reveal a mechanism of *ttcsp2* cold-inducibility, the 5'-UTR of *ttcsp2* mRNA was determined and the secondary structure in the 5'-UTR was predicted. Interestingly, the result showed that the second hairpin structure in the 5'-UTR formed after cold shock (45˚C), unlike before cold shock (70˚C). This hypothesized that *ttcsp2* mRNA was stabilized by temperature-dependent hairpin structure in the cell at low temperature. To confirm this hypothesis, I investigated *ttcsp2* mRNA abundance in the deletion mutant strain of TTHA0252 at 70˚C. Consequently, *ttcsp2* mRNA abundance increased in this mutant strain. This supported that the possibility that *ttcsp2* mRNA is down-regulated at 70˚C by TTHA0252.

The induction of *ttcsp2* mRNA occurred immediately (30 s) after temperature downshift. However, ttCSP2 protein expression was first observed at 30 min after temperature downshift. This suggested that there was a time lag between *ttcsp2* mRNA and ttCSP2 protein expression. According to the predicted secondary structure in 5'-UTR of *ttcsp2* mRNA at 45˚C, this time lag was suggested to be due to SD-like sequence sequestered in the second hairpin structure. Thus, the second hairpin structure forming at 45˚C probably regulates the expression of *ttcsp2* at post-transcriptional level. This may result in translational inhibition.

Growth analysis of double disruptant indicated that *ttcsp1* and *ttcsp2* were necessary for normal growth at 45˚C. Also, that of single disruptant suggested that ttCSP1 could compensate for the lack of ttCSP2 and *vice versa* under cold condition. DNA microarray of Δ*ttcsp2* showed the candidates of target genes regulated by ttCSP2 such as cell wall /

membrane biogenesis (M, *ttha0641-0648*), survival proteins (*ttha0360-0363*) and amino acid transporter (*ttha0447-0452*). These genes compose each series of operon.

Nucleotide binding assay revealed that ttCSP1 bound to ssDNA forming secondary structure more strongly than ttCSP2. Melting activity against dsDNA was observed only in ttCSP1. The electron potential map of ttCSP1 and ttCSP2 structures indicated that ttCSP1 had the positive-charge region to recognize stem-loop structure of ssDNA, whereas ttCSP2 did not. Our results suggest that both ttCSP1 and ttCSP2 act as an RNA chaperone, but ttCSP1 also functions as a transcription antiterminator.

In conclusion, ttCSP1 and ttCSP2 can complement each other though they have different cold-inducibility. Also, ttCSP1 was similar to ttCSP2 in DNA-binding affinity. Thus, considering that intracellular mRNAs frequently form secondary structure as temperature increase, ttCSP2 probably assist RNA chaperone activity of ttCSP1 at low temperature. These findings must be a first step to understand the molecular mechanism of cold adaptation in all organisms.

References

Agari, Y., Kashihara, A., Yokoyama, S., Kuramitsu, S., and Shinkai, A. (2008) Global gene expression mediated by *Thermus thermophilus* SdrP, a CRP/FNR family transcriptional regulator. *Mol. Microbiol.* **70**: 60-75.

Aguilar, P.S., Cronan, J.E.Jr., and de Mendoza, D. (1998) A *Bacillus subtilis* gene induced by cold shock encodes a membrane phospholipid desaturase. *J. Bacteriol.* **180**: 2194-2200.

Awano, N., Inouye, M., and Phadtare, S. (2008) RNase activity of polynucleotide phosphorylase Is critical at low temperature in *Escherichia coli* and is complemented by RNase II. *J. Bacteriol.* **190**: 5924-5933.

Bae, W., Xia, B., Inouye, M., and Severinov, K. (2000) *Escherichia coli* CspA-family RNA chaperones are transcription antiterminators. *Proc. Natl. Acad. Sci. USA* **97**: 7784-7789.

Beckering, C.L., Steil, L., Weber, M.H.W., Volker, U., and Marahiel, M.A. (2002) Genomewide transcriptional analysis of the cold shock response in *Bacillus subtilis*. *J. Bacteriol.* **184**: 6395-6402.

Dawson, W., Fujiwara, K., Kawai, G., Futamura, Y., and Yamamoto, K. (2006) A method for finding optimal RNA secondary structures using a new entropy model (vsfold). *Nucleosides Nucleotides Nucleic Acids* **25**: 171-189.

Eftink, M.R. (1997) Fluorescence methods for studying equilibrium macromolecule-ligand interactions. *Methods Enzymol.* **278**: 221-257.

Etchegaray, J.P., Jones, P.G., and Inouye, M. (1996) Differential thermoregulation of two highly homologous cold-shock genes, *cspA* and *cspB*, of *Escherichia coli*. *Genes Cells* **1**: 171-178.

Giuliodori, A.M., Di Pietro, F., Marzi, S., Masquida, B., Wagner, R., Romby, P., Gualerzi,

C.O., and Pon, C.L. (2010) The cspA mRNA Is a Thermosensor that Modulates Translation of the Cold-Shock Protein CspA. *Mol. Cell* **37**: 21-33.

Graumann, P., and Marahiel, M.A. (1996) Some like it cold: response of microorganisms to cold shock. *Arch. Microbiol.* **166**: 293-300.

Gualerzi, C.O., Giuliodori, A.M., and Pon, C.L. (2003) Transcriptional and post-transcriptional control of cold-shock genes. *J. Mol. Biol.* **331**: 527-539.

Hankins, J.S., Zappavigna, C., Prud'homme-Genereux, A., and Mackie, G.A. (2007) Role of RNA structure and susceptibility to RNase E in regulation of a cold shock mRNA, cspA mRNA. *J. Bacteriol.* **189**: 4353-4358.

Hashimoto, Y., Yano, T., Kuramitsu, S., and Kagamiyama, H. (2001) Disruption of *Thermus thermophilus* genes by homologous recombination using a thermostable kanamycin-resistant marker. *FEBS Lett.* **506**: 231-234.

Horn, G., Hofweber, R., Kremer, W., and Kalbitzer, H. (2007) Structure and function of bacterial cold shock proteins. *Cell. Mol. Life Sci.* **64**: 1457-1470.

Hoseki, J., Yano, T., Koyama, Y., Kuramitsu, S., and Kagamiyama, H. (1999) Directed evolution of thermostable kanamycin-resistance gene: a convenient selection marker for *Thermus thermophilus*. *J. Biochem.* **126**: 951-956.

Hunger, K., Beckering, C.L., Wiegeshoff, F., Graumann, P.L., and Marahiel, M.A. (2006) Cold-induced putative DEAD box RNA helicases CshA and CshB are essential for cold adaptation and interact with cold shock protein B in *Bacillus subtilis*. *J. Bacteriol.* **188**: 240-248.

Ishikawa, H., Nakagawa, N., Kuramitsu, S., and Masui, R. (2006) Crystal Structure of TTHA0252 from *Thermus thermophilus* HB8, a RNA Degradation Protein of the Metallo-β-lactamase Superfamily. *J. Biochem.* **140**: 535-542.

Jiang, W., Hou, Y., and Inouye, M. (1997) CspA, the major cold-shock protein of *Escherichia coli*, is an RNA chaperone. *J. Biol. Chem.* **272**: 196-202.

Johnston, D., Tavano, C., Wickner, S., and Trun, N. (2006) Specificity of DNA binding and dimerization by CspE from *Escherichia coli*. *J. Biol. Chem.* **281**: 40208-40215.

Kabsch, W., Kabsch, H., and Eisenberg, D. (1976) Packing in a new crystalline form of glutamine synthetase from *Escherichia coli*. *J. Mol. Biol.* **100**: 283-291.

Lee, S.J., Xie, A., Jiang, W., Etchegaray, J.P., Jones, P.G., and Inouye, M. (1994) Family of the major cold-shock protein, CspA (CS7.4), of *Escherichia coli*, whose members show a high sequence similarity with the eukaryotic Y-box binding proteins. *Mol. Microbiol.* **11**: 833-839.

Li, C., Ichikawa, J.K., Ravetto, J.J., Kuo, H.C., Fu, J.C., and Clarke, S. (1994) A new gene involved in stationary-phase survival located at 59 minutes on the *Escherichia coli* chromosome. *J. Bacteriol.* **176**: 6015-6022.

Lohman, T.M., and Bujalowski, W. (1991) Thermodynamic methods for model-independent determination of equilibrium binding isotherms for protein-DNA interactions: spectroscopic approaches to monitor binding. *Methods Enzymol.* **208**: 258-290.

Lopez, M.M., Yutani, K., and Makhatadze, G.I. (1999) Interactions of the major cold shock protein of *Bacillus subtilis* CspB with single-stranded DNA templates of different base composition. *J. Biol. Chem.* **274**: 33601-33608.

Max, K.E.A., Zeeb, M., Bienert, R., Balbach, J., and Heinemann, U. (2006) T-rich DNA single strands bind to a preformed site on the bacterial cold shock protein Bs-CspB. *J. Mol. Biol.* **360**: 702-714.

Max, K.E.A., Zeeb, M., Bienert, R., Balbach, J., and Heinemann, U. (2007) Common mode of DNA binding to cold shock domains. Crystal structure of hexathymidine bound to the

domain-swapped form of a major cold shock protein from *Bacillus caldolyticus*. *FEBS J.* **274**: 1265-1279.

Morita, M., Kanemori, M., Yanagi, H., and Yura, T. (1999a) Heat-Induced Synthesis of sigma 32 in *Escherichia coli*: Structural and Functional Dissection of *rpoH* mRNA Secondary Structure. *J. Bacteriol.* **181**: 401-410.

Morita, M.T., Tanaka, Y., Kodama, T.S., Kyogoku, Y., Yanagi, H., and Yura, T. (1999b) Translational induction of heat shock transcription factor sigma32: evidence for a built-in RNA thermosensor. *Genes Dev.* **13**: 655-665.

Mura, C., Katz, J.E., Clarke, S.G., and Eisenberg, D. (2003) Structure and Function of an Archaeal Homolog of Survival Protein E (SurEα): An Acid Phosphatase with Purine Nucleotide Specificity. *J. Mol. Biol.* **326**: 1559-1575.

Nakaminami, K., Karlson, D.T., and Imai, R. (2006) Functional conservation of cold shock domains in bacteria and higher plants. *Proc. Natl. Acad. Sci. USA* **103**: 10122-10127.

Narberhaus, F., Waldminghaus, T., and Chowdhury, S. (2006) RNA thermometers. *FEMS Microbiol. Rev.* **30**: 3-16.

Ooga, T., Ohashi, Y., Kuramitsu, S., Koyama, Y., Tomita, M., Soga, T., and Masui, R. (2009) Degradation of ppGpp by Nudix pyrophosphatase modulates the transition of growth phase in the bacterium *Thermus thermophilus*. *J. Biol. Chem.* **284**: 15549-15556.

Phadtare, S., Inouye, M., and Severinov, K. (2002a) The nucleic acid melting activity of *Escherichia coli* CspE is critical for transcription antitermination and cold acclimation of cells. *J. Biol. Chem.* **277**: 7239-7245.

Phadtare, S., Tyagi, S., Inouye, M., and Severinov, K. (2002b) Three amino acids in *Escherichia coli* CspE surface-exposed aromatic patch are critical for nucleic acid melting activity leading to transcription antitermination and cold acclimation of cells. *J.*

Biol. Chem. **277**: 46706-46711.

Phadtare, S. (2004) Recent developments in bacterial cold-shock response. *Curr. Issues Mol. Biol.* **6**: 125-136.

Phadtare, S., and Severinov, K. (2005) Nucleic acid melting by *Escherichia coli* CspE. *Nucleic Acids Res.* **33**: 5583-5590.

Reid, K.L., Rodriguez, H.M., Hillier, B.J., and Gregoret, L.M. (1998) Stability and folding properties of a model -sheet protein, *Escherichia coli* CspA. *Protein Sci.* **7**: 470-479.

Schagger, H., and von Jagow, G. (1987) Tricine-sodium dodecyl sulfate-polyacrylamide gel electrophoresis for the separation of proteins in the range from 1 to 100 kDa. *Anal. Biochem.* **166**: 368-379.

Shinkai, A., Kira, S., Nakagawa, N., Kashihara, A., Kuramitsu, S., and Yokoyama, S. (2007) Transcription activation mediated by a cyclic AMP receptor protein from *Thermus thermophilus* HB8. *J. Bacteriol.* **189**: 3891-3901.

Storey, J.D., and Tibshirani, R. (2003) Statistical significance for genomewide studies. *Proc. Natl. Acad. Sci. USA* **100**: 9440-9445.

Tanabe, H., Goldstein, J., Yang, M., and Inouye, M. (1992) Identification of the promoter region of the *Escherichia coli* major cold shock gene, cspA. *J. Bacteriol.* **174**: 3867-3873.

Thompson, J.D., Higgins, D.G., and Gibson, T.J. (1994) CLUSTAL W: improving the sensitivity of progressive multiple sequence alignment through sequence weighting, position-specific gap penalties and weight matrix choice. *Nucleic Acids Res.* **22**: 4673-4680.

Uppal, S., Rao Akkipeddi, V.S.N., and Jawali, N. (2008) Posttranscriptional regulation of cspE in *Escherichia coli*: involvement of the short 5'-untranslated region. *FEMS*

Microbiol. Lett. **279**: 83-91.

Wang, N., Yamanaka, K., and Inouye, M. (1999) CspI, the ninth member of the CspA family of *Escherichia coli*, is induced upon cold shock. *J. Bacteriol.* **181**: 1603-1609.

Xia, B., Ke, H., and Inouye, M. (2001) Acquirement of cold sensitivity by quadruple deletion of the *cspA* family and its suppression by PNPase S1 domain in *Escherichia coli*. *Mol. Microbiol.* **40**: 179-188.

Yamanaka, K., Mitani, T., Ogura, T., Niki, H., and Hiraga, S. (1994) Cloning, sequencing, and characterization of multicopy suppressors of a mukB mutation in *Escherichia coli*. *Mol. Microbiol.* **13**: 301-312.

Yamanaka, K., and Inouye, M. (1997) Growth-phase-dependent expression of cspD, encoding a member of the CspA family in *Escherichia coli*. *J. Bacteriol.* **179**: 5126-5130.

Yamanaka, K., Fang, L., and Inouye, M. (1998) The CspA family in *Escherichia coli* multiple gene duplication for stress adaptation. *Mol. Microbiol.* **27**: 247-255.

Acknowledgements

I would like to express great appreciation to Professor Seiki Kuramitsu and Drs. Ryoji Masui and Noriko Nakagawa for their guidance and many valuable discussions. I also would like to express my great appreciation to Professors Satoru Kawamura, Akihiko Ogura and Katsuyuki Tanizawa for critical advices in this study. I also wish to thank Dr. Akeo Shinkai for many valuable comments in DNA microarray analysis and Yoshihiro Agari for his assistance and discussions in statistical analysis of DNA microarray data. I wish to thank Dr. Kenji Fukui for his help with measurements of DNA microarray. I wish to thank Hirofumi Omori for technical assistance in DNA sequencing of the recombinant enzymes in this study. I wish to thank Yoshinori Koyama for providing pHG305.

Finally, I thank my colleagues in Kuramitsu laboratory, my friends and my family for their kind help and encouragements.

List of publications

Mega R., Kondo N., Nakagawa N., Kuramitsu S. and Masui R. (2009) Two dNTP triphosphohydrolases from *Pseudomonas aeruginosa* possess diverse substrate specificities. *FEBS J.* **276**, 3211-3221

Ihara, M., Okajima, T., Yamashita, A., Oda, T., Hirata, K., Nishiwaki, H., Morimoto, T., Akamatsu, M., Ashikawa, Y., Kuroda, S., Mega, R., Kuramitsu, S., Sattelle, D.B. and Matsuda, K. (2008) Crystal structures of *Lymnaea stagnalis* AChBP in complex with neonicotinoid insecticides imidacloprid and clothianidin. *Invert. Neurosci*. **8**, 71-81